Comparative Assessment of Aquifer Vulnerability near Major Dumpsites Around Karu-Abuja and Keffi Using Integrated Geophysical Methods in Nasarawa State, Nigeria

ABSTRACT

This study investigates aquifer vulnerability to leachate infiltration near major dumpsites in Karu-Abuja and Keffi, Nasarawa State, Nigeria, using integrated geophysical methods – Vertical Electrical Sounding (VES), 2-D Electrical Resistivity Tomography (ERT), Self-Potential (SP), and Very Low Frequency Electromagnetic (VLF-EM). The study area spans basement complex and sedimentary formations. Data were collected from nine VES points, four ERT profiles, ten SP profiles and sixteen VLF transverses using Ohmega Allied resistivity meter and a Gem VLF receiver. The measurements identified groundwater saturation zones and contamination pathways such as fractures and faults. Data interpretation employed tools such as WINRESIST, RES2DINV, GRAPHER, SURFER and KHFFILT. Results delineated five to six geoelectric layers, including, topsoil, clayey sand, weathered/fractured, and fresh bedrocks. Keffi's topsoil resistivity values (47.1-224.2 Ω.m, in depths ≥ 2.1 m) indicate thicker overburden and better aquifer protective layers compared to Karu-Abuja's resistivity values (16.5-294.0 Ω.m, in depths ≥ 0.5 m). Leachate infiltration is observed in both areas, with materials of low resistivity values ranging from (7.2 to 9.9 Ω.m, in depths ≥ 7.7 m) and (2.8 to 9.6 Ω.m, in depths ≥ 6.37 m) in Karu-Abuja and Keffi study areas respectively, interpreted as contaminated zones. Negative SP anomalies ranging from (– 339.9 to -1.1 mV) and (-135 to -1.65 mV) attributed to electro-kinetic reactions, and high positive VLF current-density ranging from (5 to 10 %, in depths ≥ 14 m), further corroborated contamination pathways. The study evaluated the Aquifer Protective Capacities (APC) of Keffi and Karu-Abuja, revealing that Keffi showed better protection compared to Karu-Abuja, with Keffi showing poor rating of 66%; along VES 1 (0.043 S), VES 4 (0.05 S), VES 5 (0.01 S) and VES 6 (0.02 S) and a moderate rating of 33.33 %, along VES 3 (0.29 S) and VES 4 (0.33 S). Only VES 2 (0.89), representing 16.6%, had a good rating. The Karu-Abuja study area showed poor APC rating of 66.6%, along VES 1 (0.0063 S) and VES 3 (0.002 S), and a weak rating of 33.3% along VES 2 (0.1 S). The findings emphasise the need for regular Environmental Impact Assessments (EIAs) and the installation of geo-synthetic clay liners at dumpsite bases to safeguard groundwater resources.

Keywords: Leachate, aquifer vulnerability, aquifer protective capacity, resistivity, self-potential

1. INTRODUCTION

Aquifer vulnerability refers to the susceptibility of groundwater systems to contamination and their capacity for natural water purification, which is influenced by the protective ability of overlying strata and the potential introduction of pollutants from surface sources such as leachate, industrial wastewater, landfills, and chemical fertilizers (Arthur, 2024; Nataraj, 2024). Open dumpsites are particularly significant contributors to groundwater contamination. They release pollutants through slow anaerobic decomposition, generating leachate, landfill gases,

heavy metals, and other hazardous substances (Koliyabandara *et al.,* 2024; Abdel-Shafy *et al.,* 2024).These pollutants infiltrate aquifers through advection, molecular diffusion, mechanical dispersion, and adsorption mechanisms (Wei *et al.,* 2024). Groundwater is widely considered a more sustainable and reliable source of potable water than surface water due to its natural filtration through soil and rock formations, effectively removing sediments and micro-organisms (Udosen *et al.,* 2024). However, areas with thin or permeable overburden layers, particularly where aquifers are hydraulically connected to the surface, are highly vulnerable to surface pollution. The composition and mineralogy of soil and rock significantly affect their filtration capacity. For example, highly fractured rocks like granite and limestone facilitate rapid contaminant flow, limiting purification, whereas impermeable formations like shale can provide better protection (Servin Vega, 2024; Udosen *et al.,* 2024).The increasing reliance on groundwater for domestic, agricultural, and industrial purposes in regions like Karu-Abuja and Keffi, Nasarawa State, Nigeria, underscores the importance of sustainable groundwater management. These areas are part of the Basement Complex of Nigeria, characterised by highly heterogeneous geology, which includes migmatite gneisses, schist belts, granitic rocks, and sedimentary formations, making their aquifers particularly susceptible to contamination (Dada, 2006; Bashir, 2018). Identifying aquifer vulnerability and implementing protective measures are critical to mitigating risks and ensuring long-term water supply needs. Previous studies have evaluated the aquifer hydraulic properties and groundwater protective capacity in Abavo area, Nigeria (Chinyem and Ovwamuedo, 2024). Results from the pumping test analysis, using the Cooper Jacob's method, revealed that the transmissivity, specific capacity, storativity and hydraulic conductivity are 5.9 m^2/day, 33.13 m/day, 0.0069 and 0.1722 m/day respectively. The study revealed longitudinal conductance and transverse resistance range of 0.001048-0.027828 Ω^{-1} and 105470.4-1255775.3 $\Omega \cdot m^2$ respectively. The study established that the aquifer is semi-confined, has poor protective capacity and high rechargibility. In another study, Chinyem (2024) determined aquifer parameters and groundwater protective capacity in parts of the Nsukwa clan using geoelectric and pumping test methods. The computed *T* and *K* from geoelectric sounding ranged from 11.37 to 34.79 m^2/day, with a mean value of 18.51 m^2/day and 0.8243 m/day, respectively, while the *T* and *K* values from the pumping test are 18.58 m^2/day and 0.8251 m/day, respectively. *S* and *R* values ranged from 0.001179 to 0.0131619 Ω^{-1} and 2434 to 102,090 Ωm^2, respectively, revealing a poor aquifer protective capacity and moderate yield.

Also, Satheeshkumar (2024) employed VES method to assess the groundwater potential of Naraiyur micro-watershed. Aquifer capacity in the study area indicated low vulnerability area. Ishola (2024) employed twenty-seven (27) VES to evaluate aquifer protective capacity at Obafemi-Owode LGA, Ogun State South-West Nigeria. Results revealed that the reflection coefficient ranged between 0.02 and 0.98 while protective capacity ranged between 0.00135 and 0.510. A group of researchers probed sixteen VES stations to address potable water challenge in Shango, North-Central Nigeria (Ejepu *et al.*, 2024). The result revealed that the hydraulic conductivity ranged from 0.465 to 0.534 m/day, while transmissivity varied from 9.589 m^2/day to 26.029 m^2/day across different VES points. They concluded that regions exhibiting thick layers and low resistivity values indicate high longitudinal conductivity. Another group of researchers employed VES and 2-D ERT surveys constrained by well lithological information, to investigate leachate infiltration at a major open dump in Eket, Southern Nigeria (Udosen *et al.*, 2024). Dar-Zarrouk indices and electrical reflection co-efficient indicated that the highly heterogenous region had moderate aquifer protective capacity and moderate aquifer potentiality. The aim of this study is to evaluate and compare aquifer vulnerability near major dumpsites in Karu-Abuja and Keffi using integrated geophysical methods and to specifically delineate leachate contamination pathways, evaluate the aquifer protective capacities and determine the hydraulic characteristics of the study areas. This will provide essential data to guide waste disposal practices, safeguard groundwater resources and inform sustainable water resource management policies.

2. MATERIALS AND METHODS

Location and Geology

The two dumpsites, about 37 km apart, are in Nasarawa State, Nigeria (Fig. 1). The thirty-year-old Karu dumpsite and its control center are situated between latitudes 9°00'27.7986"N and 9°00'45.2016"N and longitudes 7°34'23.0982"E and 7°34'23.4006"E. Whereas the dumpsite at Keffi and its control center are located between latitudes 8°50'16.7994"N and 8°50'38.4822"N and longitudes 7°53'15.36"E and 7°53'2.5002"E. The drainage pattern in the area is dendritic reflecting the resistance of underlying rock units to erosion. Numerous streams and channels drain into the SE-trending River Uke (Bashir, 2018).The region experiences two major climatic conditions: a rainy season from April to October, with a peak in August, and a dry season from

February to mid-April. The annual rainfall averages 1357 mm. Harmattan winds, characterized by dry and dusty conditions, occur from November to January. Temperatures in the area range from 26.58°C to 32.51°C. High temperatures are recorded between February and May, while cooler temperatures, averaging 26.78°C, dominate from July to September during the rainy season. The highest temperatures, around 34°C, occur during the dry season (November to March). Rainy season temperatures drop to approximately 24°C due to dense cloud cover (McCurry, 1985). The area's annual rainfall ranges from 1100 mm to 1600 mm (Ajibade and Wright, 1988). Figure 2 shows the geology of both dumpsites. The Karu dumpsite is underlain by Muscovite Schist while the Keffi dumpsite in over Migmatite. The formations are part of the north-central Basement Complex of Nigeria, bearing the imprints of multiple orogenic events, including the Liberian (2700 ± 200 Ma), Eburnean (2000 ± 200 Ma), and Pan-African (600 Ma) events (Oversby, 1975). The lithologic units exhibit polycyclic deformation, resulting in prominent structures such as joints, foliations, and faults (Dada, 2006). The dominant structures display NNE-SSW trending gneissose foliations, with occasional ENE-WSW and NNW-SSE trends and dip angles ranging from 6° to 60° in the SE direction (Tanko *et al.*, 2015).

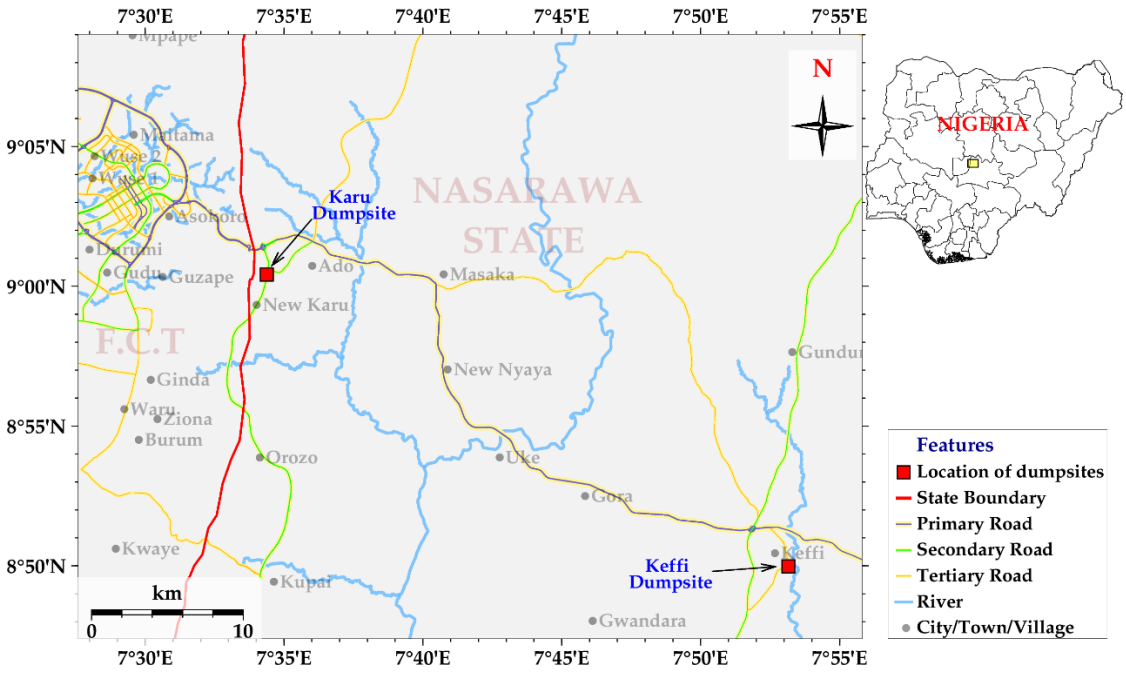

Figure 1: Location of study areas (red squares).

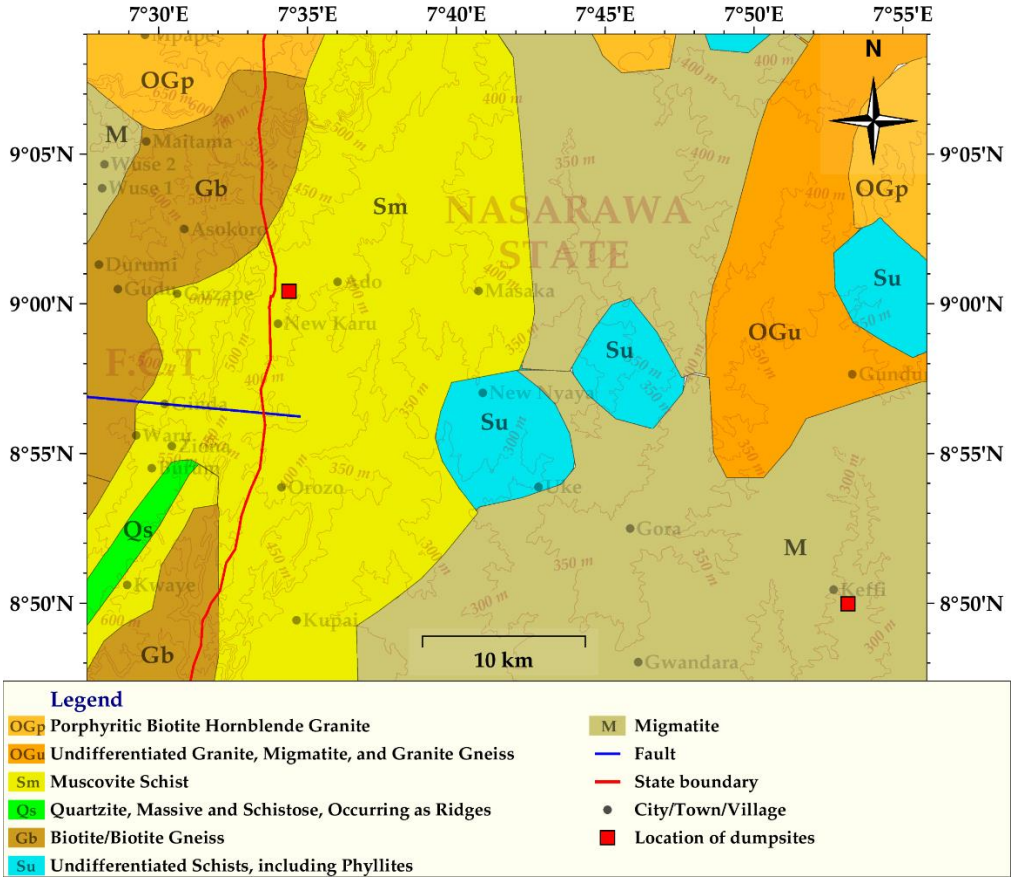

Figure 2: Geological map of the study areas (after NGSA, 2019)

The Ohmega Allied resistivity metre and its accessories, hammer, electrodes/non-polarizable, measuring tape, cables, reels, Global Positioning System (GPS) and a portable GEM VLF receiver were used to obtain VES, 2-D ERT, SP and VLF-EM data. Nine (9) VES points with maximum current electrode spacing (AB/2) of 170 m using Schlumberger array configuration, four (4) 2-D ERT profiles at constant electrode spacing of 5 to 120 m using Wenner array configuration, nine (9) SP profiles at constant electrode spacing of 5 to 170 m, and sixteen (16) VLF-EM profiles at 5 m intervals and a maximum spacing of 100 m, were established at the dumpsite. Data were also collected at the control centre located about 700 m away from the dumpsite by constraining each of the method along the same transverse. The VLF-EM data was collected using a portable GEM VLF receiver within the frequency range of 15.1 – 24.0 kHz. Two borehole logs (Anudu *et al*., 2021; Sunkari *et al.*, 2021), obtained from a distance of 50 m away from the study areas were used to correlate with VES points along the profiles. Data

collected were interpreted using tools such as WINRESIST, RES2DINV, GRAPHER, SURFER and KHFILT. KHFILT was utilized for filtering and mapping current densities.

2.1 Basic Operational Principles

The operational principle of the electrical resistivity method is the Ohm's law given as:

$$V=IR \qquad 1$$

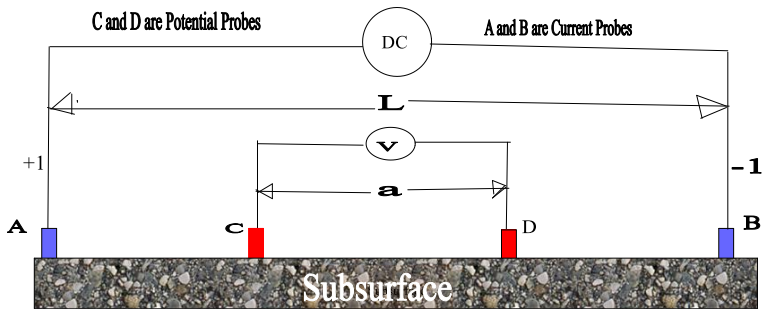

Figure 3: Schlumberger configuration

Where V is the potential difference (V), I, the current (A) and R is the resistance (Ω).

The subsoil's reaction to the flow of current in the ground can be expressed by:

$$\rho_a = RK \qquad 2$$

Where K is a geometric factor (K-Factor) that depends on the configuration of the four electrodes shown in Fig. 3. The K-Factor can be expressed from Fig. 3 as in Eq. 3;

$$K = 2\pi\left[\left(\frac{1}{AC}-\frac{1}{CB}\right)-\left(\frac{1}{AD}-\frac{1}{BD}\right)\right]^{-1} \qquad 3$$

Considering Fig. 3, we write Eq. (4)

$$\begin{cases} AC = BD = \left(\frac{L-a}{2}\right) \\ CB = AD = \left(\frac{L+a}{2}\right) \end{cases} \qquad 4$$

Substituting (4) into (3), the geometry factor for the Conventional Schlumberger array, becomes:

$$K = 2\pi\left[\left(\frac{2}{L-a} - \frac{2}{L+a}\right) - \left(\frac{2}{L+a} - \frac{2}{L-a}\right)\right] \qquad 5$$

Equation 5, can be expressed further to obtain 6, so that

$$K = \frac{\pi}{4}\left[\frac{L^2 - a^2}{a}\right] \qquad 6$$

2.1 The Self-Potential

The self-potential method is a passive geophysical method involving the measurement of the electric potential at a set of measurement points called self-potential stations (Revil and Jardani, 2013). The sampled electrical potential (or electrical field) can be inverted to determine the causative source of current in the ground and obtain important information regarding groundwater flow, hydro-mechanical and geo-chemical disturbances. The general equation for coupled flows (Overbeek, 1952) can be written as:

$$J_i = \sum_j L_{ij} X_j \qquad 7$$

Where the fluxes J_i (of charges, matter, heat, etc.) are related to the various forces X_j (gradients of electrical potential, pressure, temperature, etc.) through the coupling coefficients L_{ij} (‘‘phenomenological coefficients’’ (de Groot and Mazur, 1983) or ‘‘conductivities’’ (Sill, 1982).

2.1.1 The VLF-EM Diagnostics

The Fraser filter transforms the zero-crossing points into peaks, enhancing the signals of the conductive structures. Plotted cross-sections show the Fraser filtered data (real or in-phase components) and the measured values (Oluwafemi and Oladunjoye, 2013). In-phase (abbreviation IP) and Quadrature (abbreviation Quad) are the two most important field measurements of the VLF method and can be expressed as the normalized real and quadrature components of the vertical magnetic field:

$$inphase = \frac{real(H_z)}{\sqrt{(H_x^2 + H_y^2)}} \qquad 8$$

$$Quad = \frac{imag(H_z)}{\sqrt{(H_x^2 + H_y^x}} \qquad 9$$

2.1.2 Estimation of Aquifer Protective Capacity (APC)

The estimation of the aquifer protective capacity is based on the values of the longitudinal unit conductance (S) of the overburden rock units (Arowoogun and Osinowo, 2022).
The total transverse resistance R is given by:

$$R = \sum_{i=1}^{n} h_i \rho_i \qquad 10$$

The total longitudinal conductance S is:

$$S = \sum_{i=1}^{n} \frac{h_i}{\rho_i} \qquad 11$$

where h_i and ρ_i are the thickness and resistivity of the i^{th} layer in the section, respectively. The longitudinal layer conductance Si can also be expressed by:

$$S = \sigma_i h_i \qquad 12$$

where h_i is the layer thickness and ρ_i is layer resistivity, while the number of layers from the surface to the top of aquifer varies from i = 1 to n (Table 1):

Table 1: Modified longitudinal conductance/protective capacity rating (Oladapo and Akintorinwa, 2007)

Longitudinal Conductance (mhos)	**Protective Capacity Rating**
>10	Excellent
5-10	Very Good
0.8-4.9	Good
0.2-0.79	Moderate
0.1-0.19	Weak
<0.1	Poor

2.3 Photographs from the field

Plate 1: Data collection at the Karu-Abuja and Keffi dumpsites (**a** and **c**) and their Control Centres (**b** and **d**) respectively.

3. RESULTS

3.1 Keffi Dumpsite, Panteka Area, Nasarawa State

The summary of results for the nine (9) VES points conducted near the Keffi and Karu-Abuja dumpsites and their control centres indicating the No. of layers, Curve Types, resistivity values (Ω.m), thicknesses (m), depth (m) and delineated lithological units are presented in Tables 2 and 3:

Table 2: Vertical Electrical Sounding data for VES stations 1-6 (Keffi)

VES	No. of Layer (s)	Curve Types	Res. (Ω.m)	Thickness	Depth	Lithological Units
1	5	HA	47.1	0.5	0.5	Topsoil (lateritic)
			9.6	4.1	4.6	Sandy clay, leachate
			116.4	5.0	9.6	Weathered basement (Medium grain sandstone)
			3061.4	42.8	52.4	Partial fresh Basement
			3144.9	-		Fresh Basement
2	5	QA	199.5	1.1	1.1	Topsoil (lateritic)

			12.8	0.6	1.7	Silty Sandy
			2.8	2.5	4.1	leachate
			1257.6	19.2	23.4	Partial fresh Basement
			3586.2	-		Fresh Basement
3	5	HA	224.2	0.8	0.8	Topsoil (lateritic)
			66.8	19.5	20.2	Sandy-clay
			1043.9	16.7	36.9	Partial fresh Basement
			6696	-		Fresh Basement
4	5	HK	113.5	2.1	2.1	Topsoil
			18.9	6.2	8.3	Sandy clay
			3371.3	19.7	28	Partial fresh Basement
			13402.7	-		Fresh Basement
5	5	HA	230.6	1.6	1.6	Topsoil (lateritic)
			78.1	26.1	27.7	Weathered basement (Medium grained sandstone)
			364.9	18	45.7	Fractured basement (Fine grained sand)
			2985.9	-		Fresh Basement
6	5	HK	125.0	1.6	1.6	Topsoil
			9.2	2.6	4.2	Sandy clay
			195.9	3.5	7.7	Weathered/fractured basement (Medium to fine grained sand)
			5384.7	35	42.7	Fresh Basement
			9152	-		Partial fresh Basement

Table 3: Vertical Electrical Sounding data for VES stations 1-3 (Karu-Abuja)

VES	No. of Layer (s)		Res	Thickness	Depth	Lithological Units
1	5	HA	294	0.6	0.6	Topsoil
			21.5	0.4	1	Weathered basement
			7.2	1	2	Weathered basement/leachate infiltrated
			221.7	1.4	3.4	Fractured basement
			57293.9			Fresh Basement
2	6	KHA	16.5	0.5	0.5	Topsoil (Lateritic)
			231.2	0.9	1.5	Weathered layer
			131.8	0.7	2.2	Weathered layer
			9.9	5.5	7.7	Weathered basement/leachate infiltrated

			346.3	35.2	43	Fractured basement
			478.8			Fractured basement
3	5	QA CC	74.4	0.7	0.7	Topsoil(Lateritic)
			21.4	2.2	2.9	Weathered basement
			11.4	5.8	8.7	Weathered basement/leachate infiltrated
			419.8	12.1	20.8	Fractured basement
			1932.6			Fresh Basement

3.2 Estimated Aquifer Parameters of the surveyed area (Keffi)

The primary aquifer parameters (resistivity and thickness) are determined from Tables 2 and 3 and are used to estimate the geo-hydraulic parameters. The summary of the Daz-Zarrouk parameters estimated for the weathered aquifers for both the Keffi and Karu-Abuja dumpsites and their control centres showing the VES points, resistivity values ρ (Ω.m), Aquifer thicknesses h (m), Electrical conductivity σ ($\Omega.m^{-1}$), Longitudinal Conductance S (mhos), Transverse Resistance T_R ($\Omega.m^{-2}$), Hydraulic conductivity K (m/day), Transmissivity T (m^2/day), Quantity of water (Q) and porosity ϕ (%) are presented in Tables 4 to 7:

Table 4: The summary of Dar-Zarrouk parameters and electrical conductivity K (m/day) estimated for the weathered aquifers in the study area (Keffi)

VES	ρ (Ω.m)	Thickness (h/m)	$\sigma = 1/\rho$ ($\Omega.m^{-1}$)	$S = \sigma h$ (mhos)	$T_R = h\rho$ ($\Omega.m^{-2}$)	K (m/day)
1	116.4	5.0	0.0086	0.0430	582.0	4.57
2	2.8	2.5	0.35714	0.8929	7.0	147.88
3	66.8	19.5	0.0150	0.2920	1302.6	7.67
4	18.9	6.2	0.0530	0.3280	117.2	24.91
5	364.9	18.0	0.0027	0.0493	6568.2	1.57
6	195.9	3.5	0.0051	0.0179	685.7	2.81

Table 5: The summary of aquifer transmissivity (T), quantity of water Q and porosity ϕ (%) estimated for the weathered aquifers in the study area (Keffi)

VES	T = kh (m^2/day)	Quantity Q = (kσ)	Porosity ϕ (%)
1	22.85	0.04	32.34
2	369.70	52.82	47.98
3	149.58	0.115	34.67
4	154.42	1.32	39.97
5	28.33	0.004	27.54
6	9.84	0.014	30.15

Table 6: The summary of Dar Zarrouk parameters and electrical conductivity K (m/day) estimated for the weathered aquifers in the study area (Karu-Abuja)

VE S	ρ (Ω.m)	Thickness (h)	σ = 1/ ρ	S = σh	R = hρ	K (m/day)
1	221.7	1.4	0.0045	0.006	310.38	2.51
2	346.3	35.2	0.0029	0.10	12189.7	1.65
3	419.8	12.1	0.0024	0.03	5079.6	1.38

Table 7: The summary of aquifer transmissivity (T), quantity of water Q and porosity ϕ (%) estimated for the weathered aquifers in the study area (Karu-Abuja)

VES	Tr = kh	Quantity (kσ)	Porosity (ϕ) (%)
1	3.51	0.0113	29.63
2	58.2	0.0048	27.76
3	16.7	0.003	26.95

3.2.1 Results of computer modeled curve for six (6) VES points (Keffi)

The results of the computer modeled curves for the nine (9) VES points conducted in Keffi and Karu-Abuja study areas are shown in Figures 4 to 12:

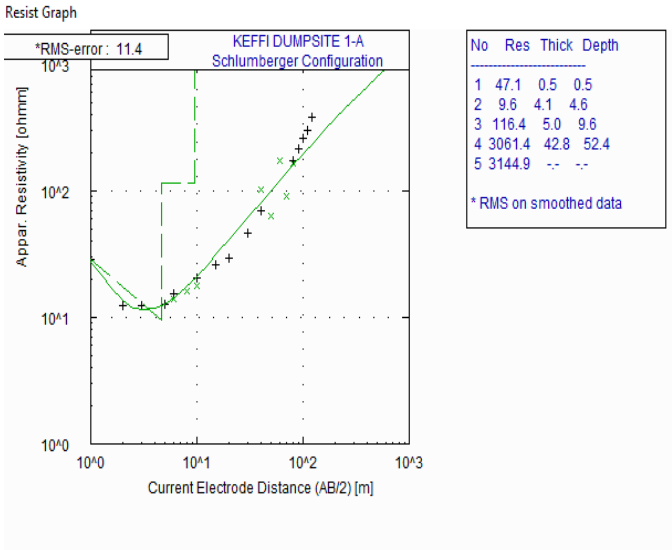

Figure 4: Results of computer modeled curve for VES 1 (Keffi)

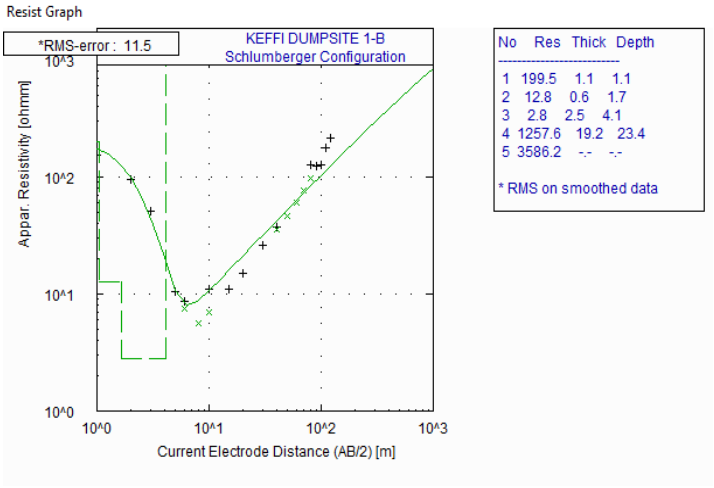

Figure 5: Results of computer modeled curve for VES 2 (Keffi)

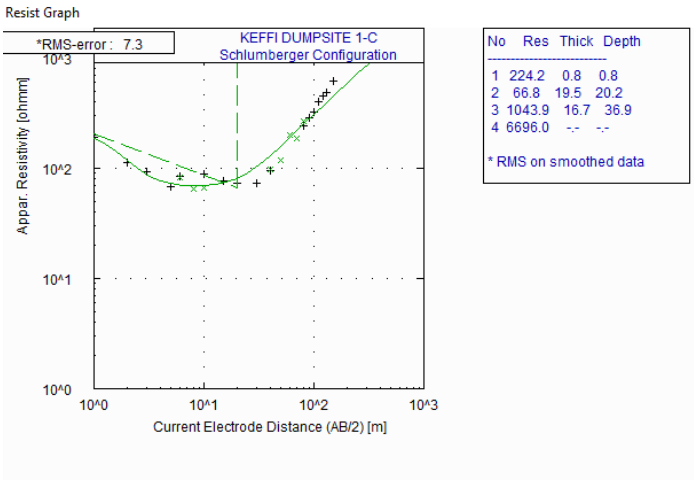

Figure 6: Results of computer modeled curve for VES 3 (Keffi)

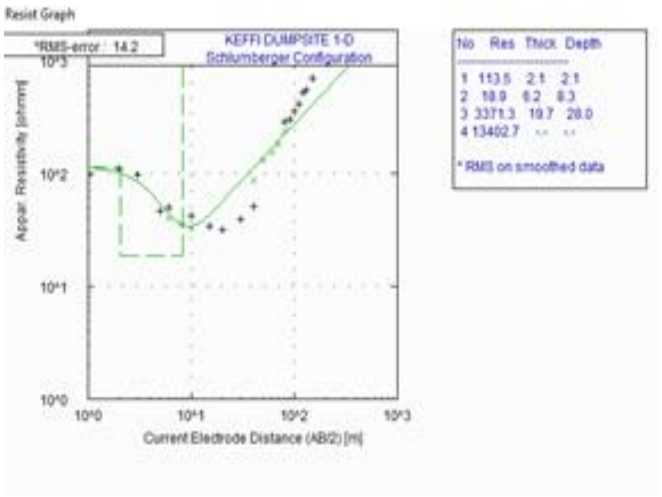

Figure 7: Results of computer modeled curve for VES 4 (Keffi)

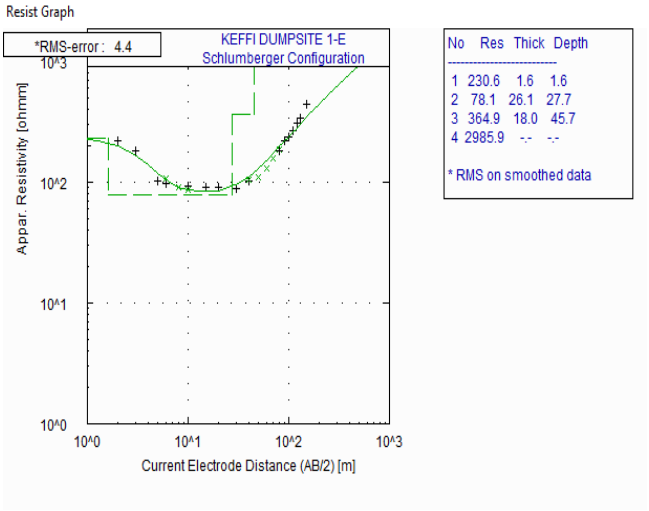

Figure 8: Results of computer modeled curve for VES 5 (Keffi)

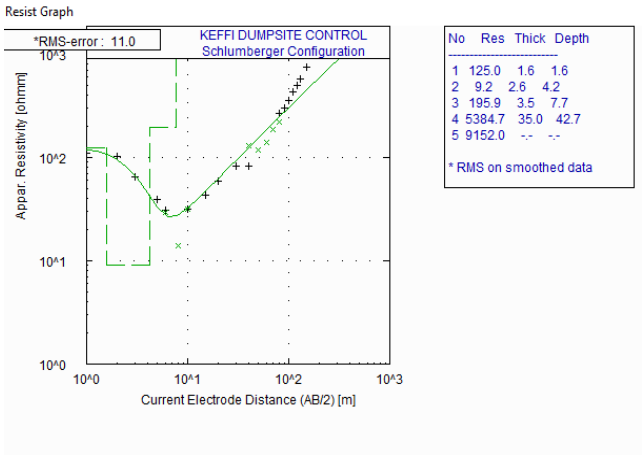

Figure 9: Results of computer modeled curve for VES 6 (Control Centre, Keffi)

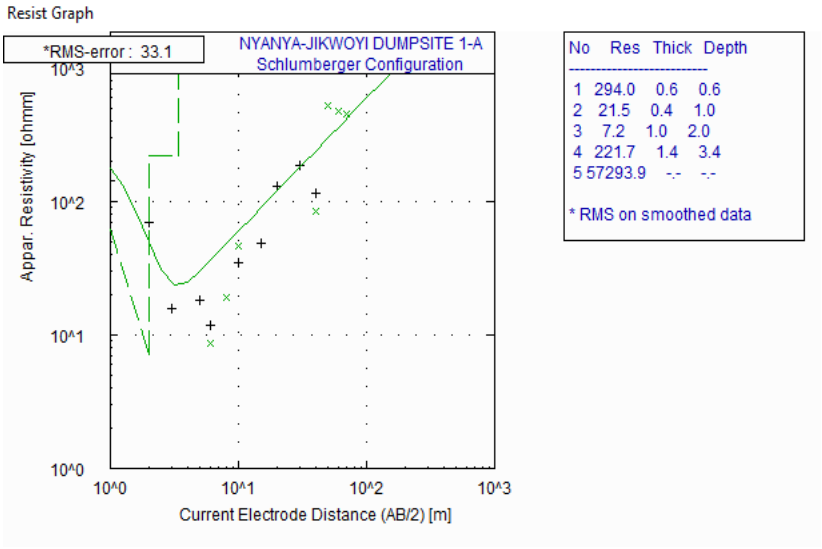

Figure 10: Results of computer modeled curve for VES 1 (Karu-Abuja)

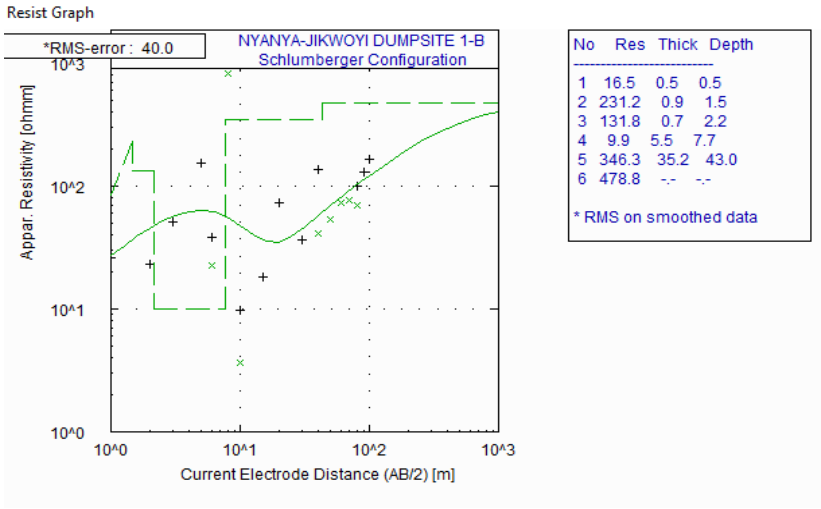

Figure 11: Results of computer modeled curve for VES 2 (Karu-Abuja)

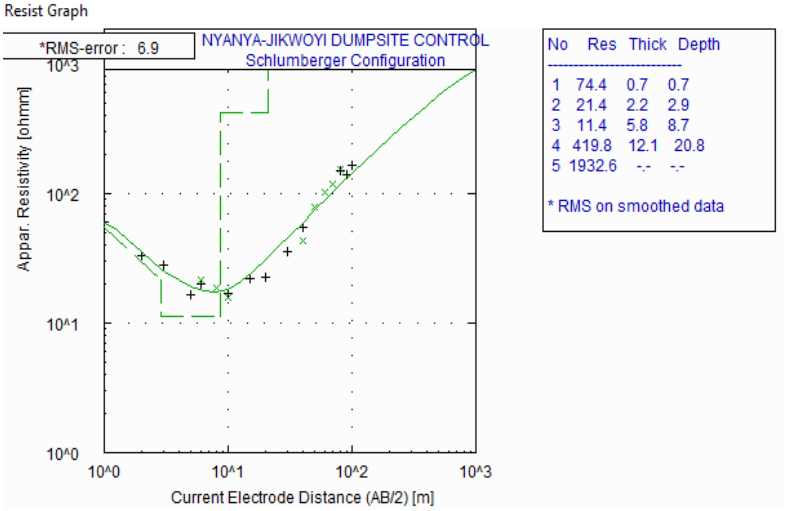

Figure 12: Results of computer modeled curve for Control Centre (Karu-Abuja)

3.2.2 Correlation of Borehole log with VES (Keffi)

The correlation of borehole lithological logs BH (D), BH (C) and BH with resistivity sounding (VES) results for Keffi and Karu-Abuja study areas are shown in Figures 13 and 14:

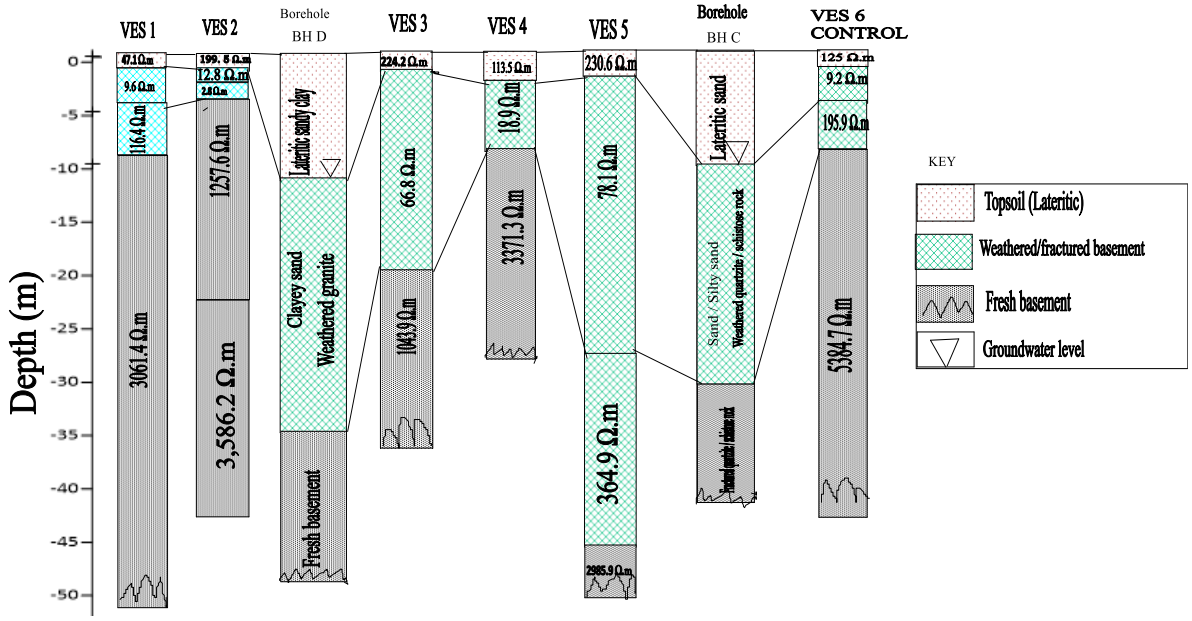

Figure 13: Correlation of resistivity sounding (VES) results with borehole lithological logs in the study area (Keffi)

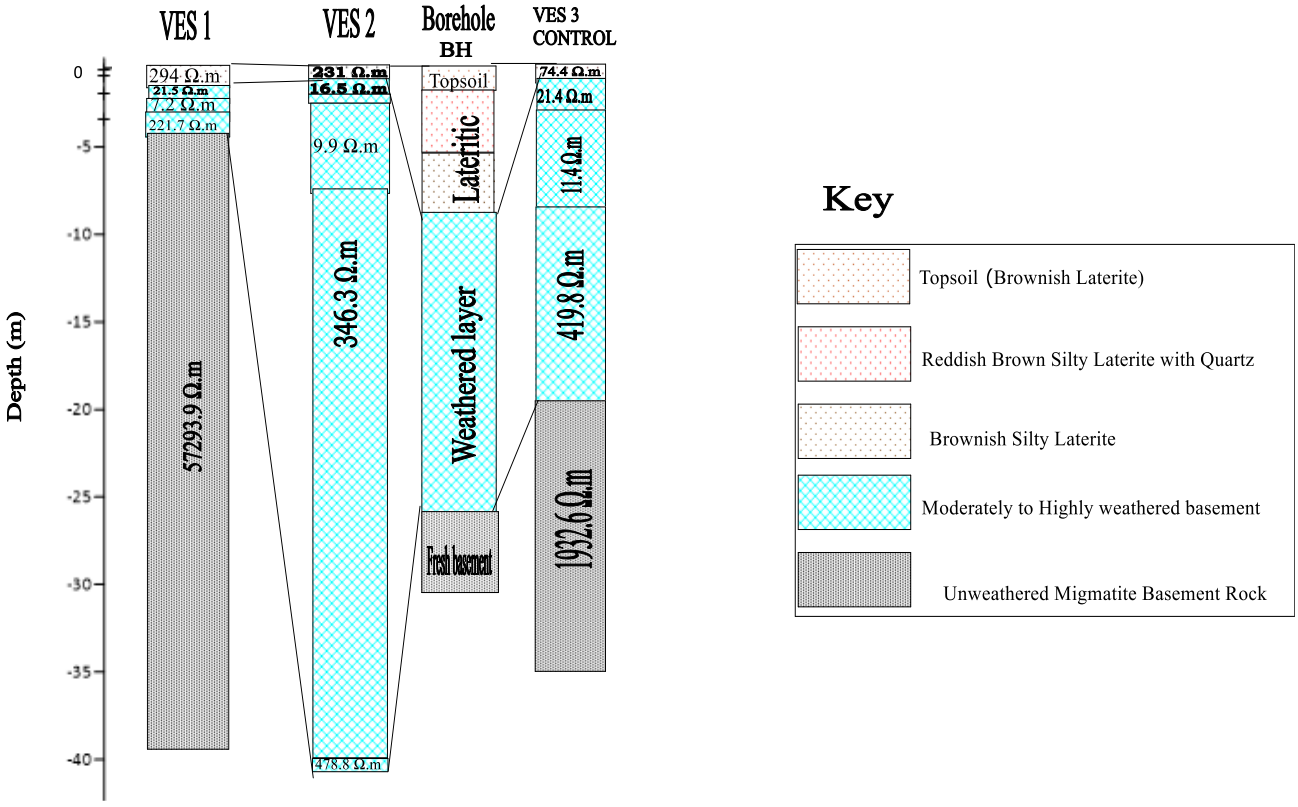

Figure 14: Correlation of resistivity sounding (VES) results with borehole lithological logs in the study area (Karu-Abuja)

3.3 Results of the Self-Potential (SP) survey conducted in the study area (Keffi)

The results of the nine (9) SP profiles conducted in Keffi and Karu-Abuja study areas are shown in Tables 8 and 9:

Table 8: Summerised results from self-potential (SP) survey in the Keffi study area

Distance X (m)	**SP (mV) LINE 1**	**SP (mV) LINE 2**	**SP (mV) LINE 3**	**SP (mV) LINE 4**	**SP (mV) LINE 5**	**SP (mV) Control Centre6**
0	-28.28	42.83	-69.06	25.51	-1.65	43.44
5	-8.32	-16.49	-75.62	21.81	-50.82	-48.98
10	-135.2	-61.89	-75.59	-49.39	-54.71	70.16
15	-103.4	-17.52	-5.08	5.164	-39.04	29.10
20	-70.08	2.79	-33.40	20.18	-73.36	3.54
25	-56.97	5.41	-57.58	19.57	467.2	-7.81
30	-79.72	92.42	-33.61	-4.447	-50.21	-14.75
35	-68.65	24.69	-54.92	-19.67	-44.26	-54.30
40	-69.47	48.36	-24.59	6.496	-29.71	1.578
45	-79.49	67.01	-23.87	31.15	-19.26	-42.83
50	-50.0	89.14	-50.82	40.57	-40.16	-53.69
55	-42.21	90.78	-93.24	66.4	-5.533	14.55
60	-23.87	91.81	-90.31	36.47	-40.16	-37.60
65	-18.85	47.13	-85.45	81.15	-28.69	-106.50
70	8.238	55.02	-22.74	9.191	-12.09	51.23
75	-14.34	68.04	-13.52	45.49	-10.96	-21.62
80	-39.24	36.17	9.04	-7.89	21.10	-13.52
85	-73.36	32.99	60.86	48.77	-46.93	57.38
90	-44.88	23.67	-24.18	43.03	-6.435	-58.81
95	-64.55	42.62	-39.96	21.51	-61.27	-79.72
100	-40.57	45.29	-1.25	-1.086	-22.33	7.623
105	1.793	45.90	-26.33	-13.01	-15.78	2.22
110	-7.623	39.34	-46.93	-7.582	-43.65	26.12
115	-24.79	84.84	-22.33	-3.463	-84.43	44.67
120	-	-	-37.91	-33.3	-80.74	85.05
125	-	-	-64.35	-3.77	-256.5	-41.10
130	-	-	-68.44	-54.51	-54.92	-3.86
135	-	-	-43.03	-	-60.86	121.90
140	-	-	-83.00	-	-43.85	85.66
145	-	-	-43.85	-	-46.52	49.80

Table 9: Summerised results from Self-Potential (SP) survey in the Karu-Abuja study area

Distance X (m)		SP (mV) 1	SP (mV) 2	SP (mV) 3	SP (mV) 4 Control
0		160.1	-206.9	-22.44	88.1
5		-338.8	-215.1	30.22	-74.4
10		-268.8	-196.8	-424.2	-56.8
15		-304.4	-191.7	20.59	-81.4
20		-326.7	-185.6	23.05	-62.7
25		-328.7	-173.5	23.36	100.5
30		-333.5	-170.4	40.16	88.9
35		328.7	-164.3	112.7	69.1
40		338.9	-142.4	1.762	56.2
45		338.9	-107.5	25.82	-87.5
50		350.0	-84.43	25.61	-174.1
55		-341.1	-98.17	65.17	-172.2
60		-344.9	-3.432	17.72	-152.6
65		-363.2	-6.64	24.08	-179.6
70		-353.1	-22.33	27.76	-131.1
75		-349.0	9.078	-3.072	-56.8
80		347.0	-5.70	-40.78	-95.7
85		337.8	42.62	-17.62	-44.5
90		337.8	35.96	-2.910	-62.3
95		-339.9	46.11	-	-

3.4 CORRELATION ANALYSIS

The following cross-sections correlates the Self Potential (mV) profiles, their corresponding SP contours and 3-D SP plots, VES transverses and 2-D ERT geo-electric sections along the survey lines in both study areas (Figures 15 – 24):

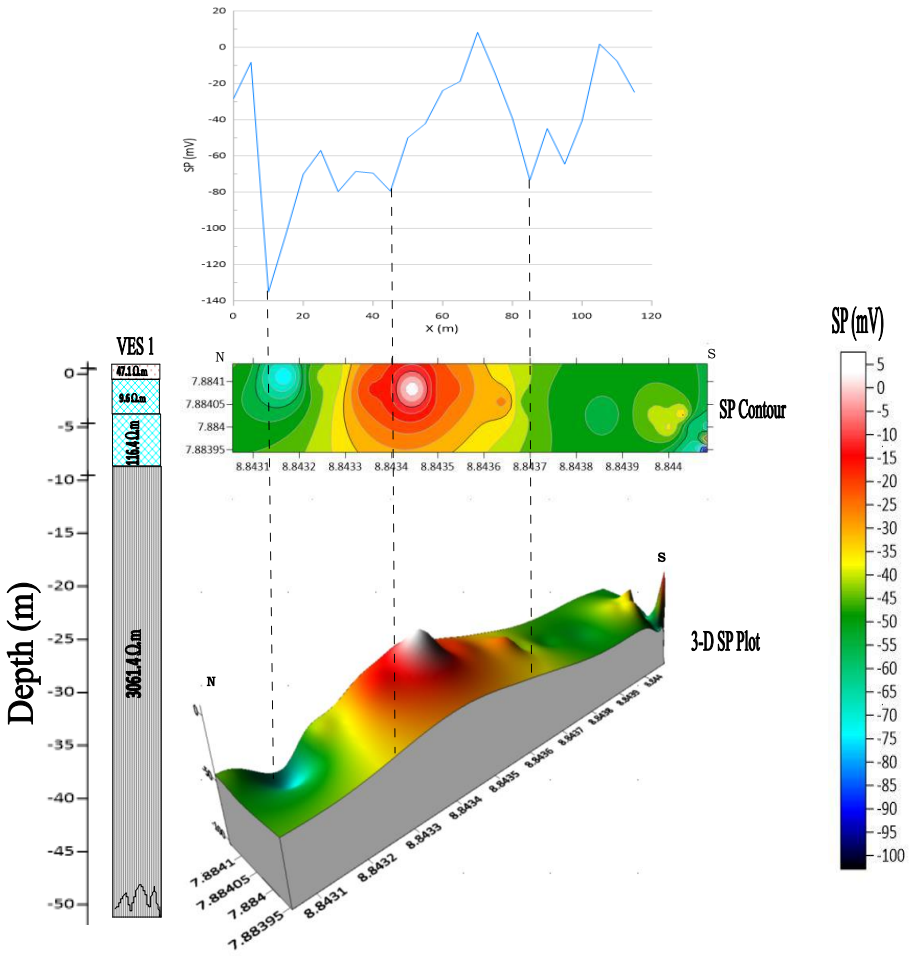

Figure 15: Cross-section correlating the VES transverse, SP signals, SP contours and 3-D SP plot and VES log along Profile 1(Keffi)

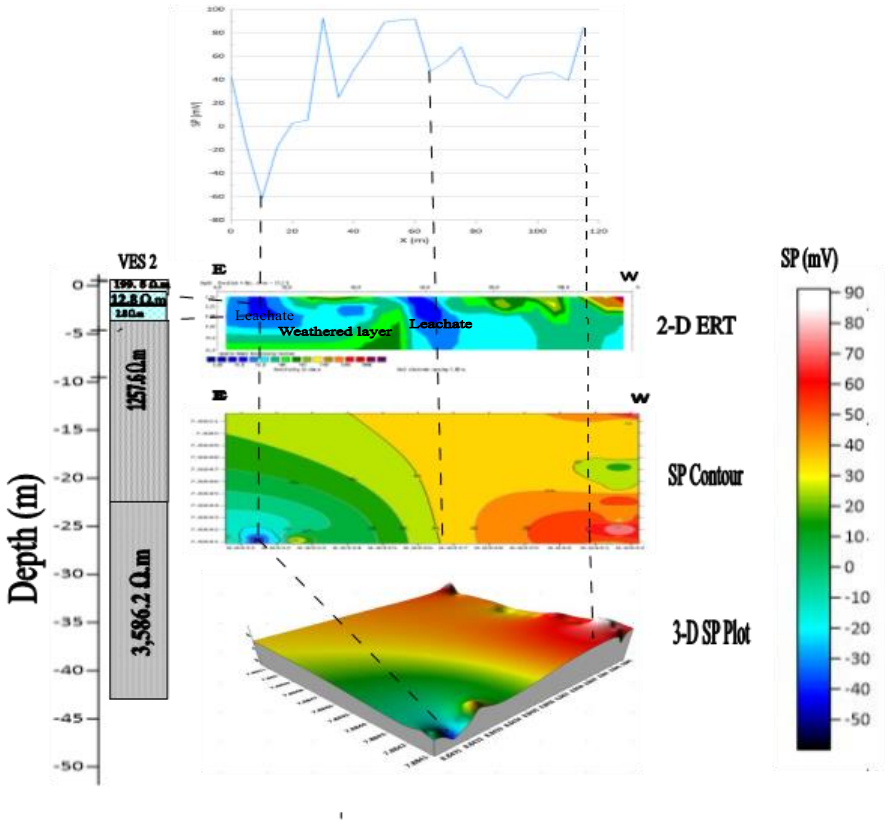

Figure 16: Cross-section correlating the 2-D ERT geo-electric section, VES transverse, Self-Potential signal, SP contour and 3-D SP plot along profile 2 (Keffi)

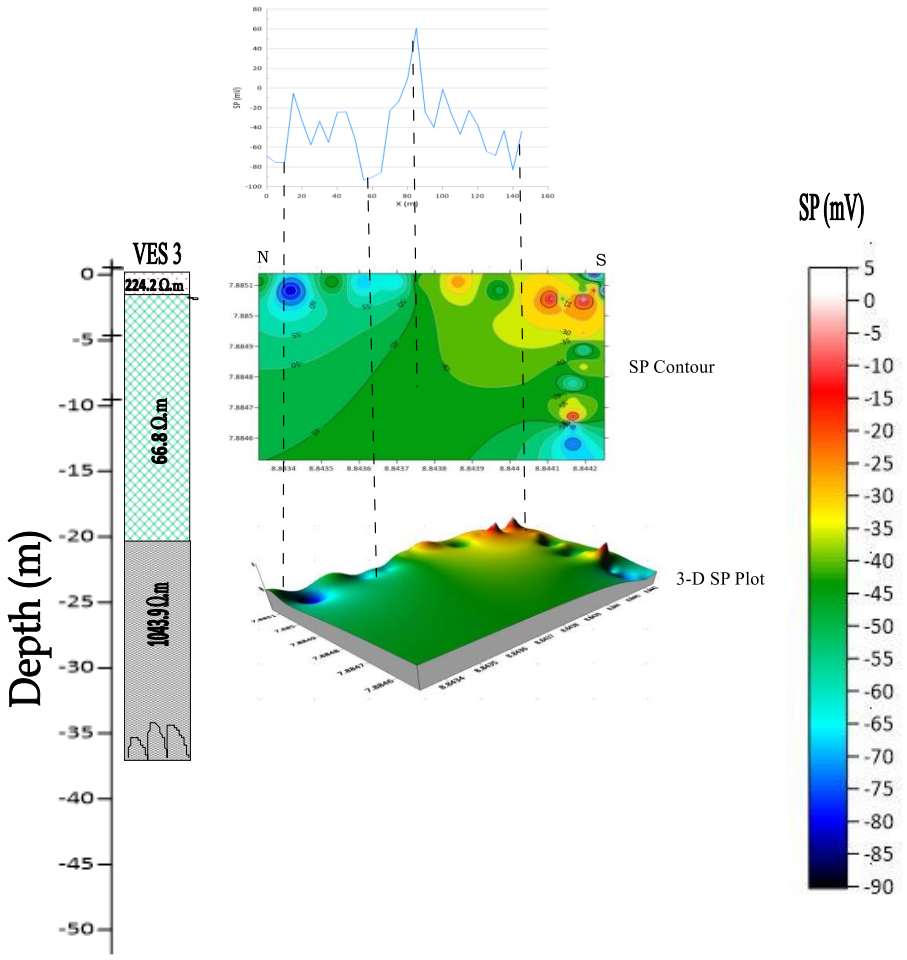

Figure 17: Cross-section correlating the VES transverse, Self-Potential signal, SP contours and 3-D SP plot along Profile 3 (Keffi)

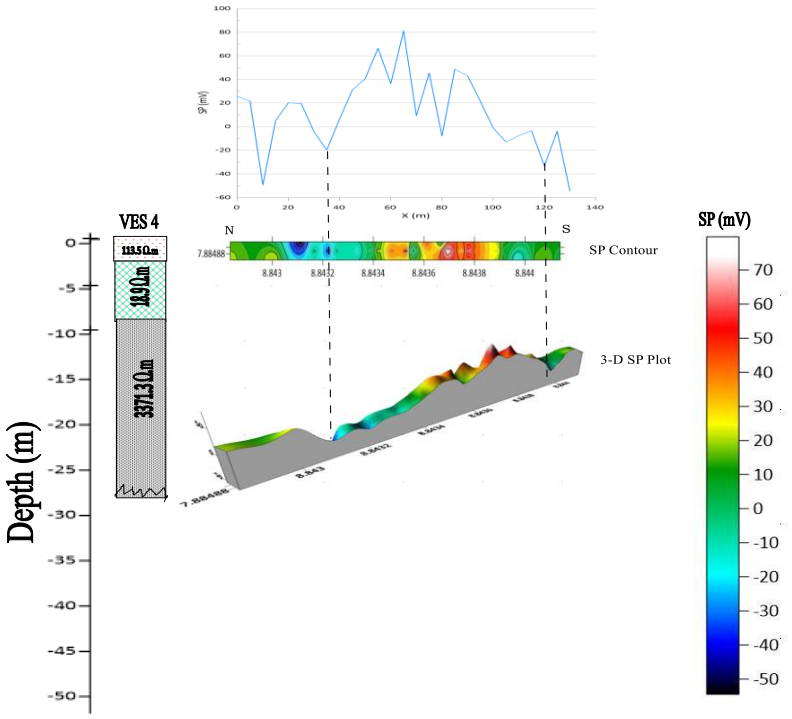

Figure 18: Cross-section correlating the VES transverse, Self-Potential signal, SP contours and 3-D SP plot along Profile 4 (Keffi)

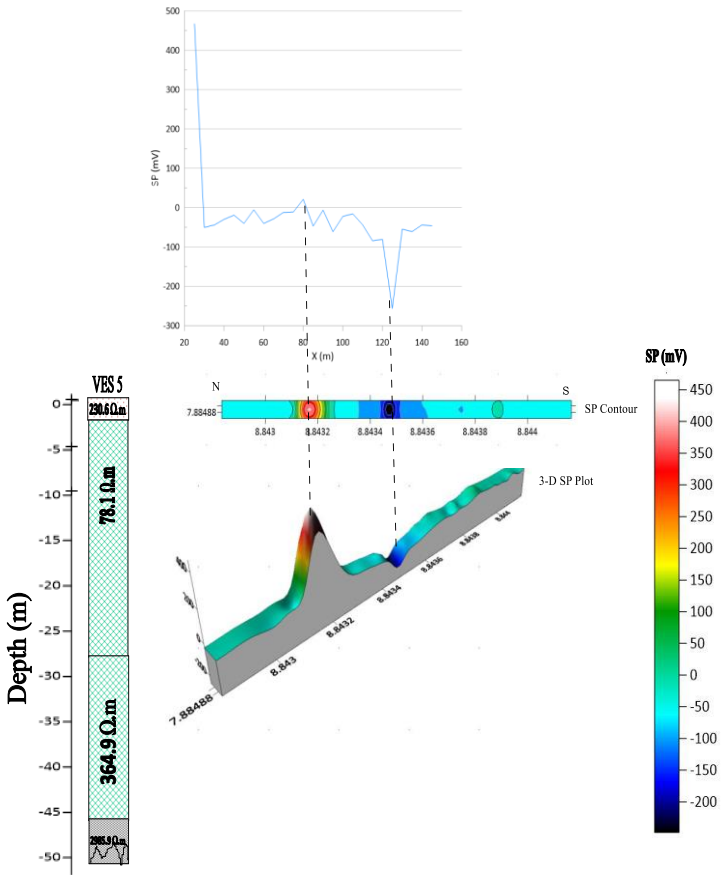

Figure 19: Cross-section correlating the VES transverse, Self-Potentialsignal, SP contours and 3-D SP plot along Profile 5 (Keffi)

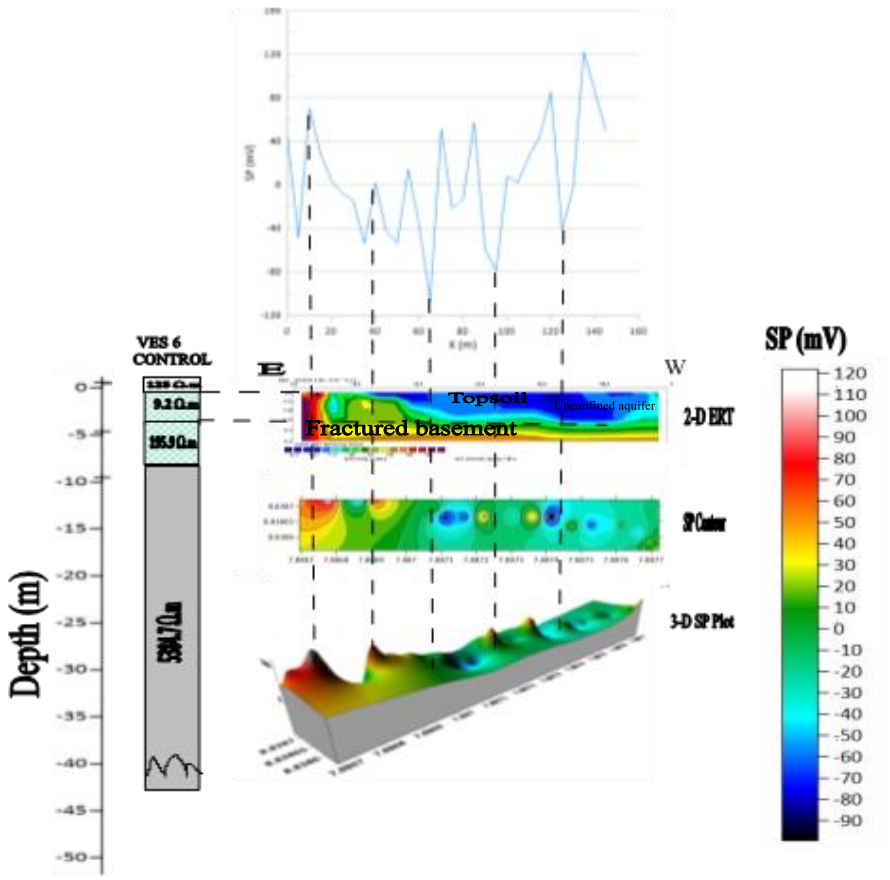

Figure 20: Cross-section correlating the 2-D ERT geo-electric section, VES transverse, Self-Potential profile, SP contour and 3-D SP plot along profile 6 (Keffi, Control Centre)

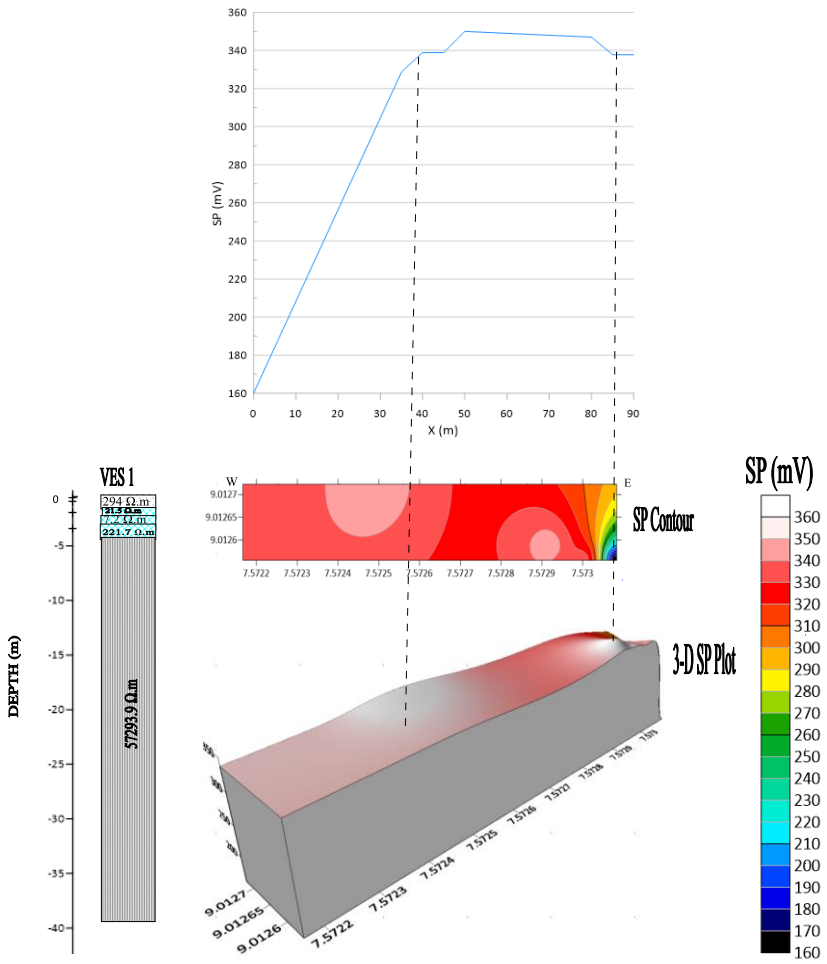

Figure 21: Cross-section correlating the SP profile, SP contours and 3-D SP plot and VES log along Profile 1 (Karu-Abuja)

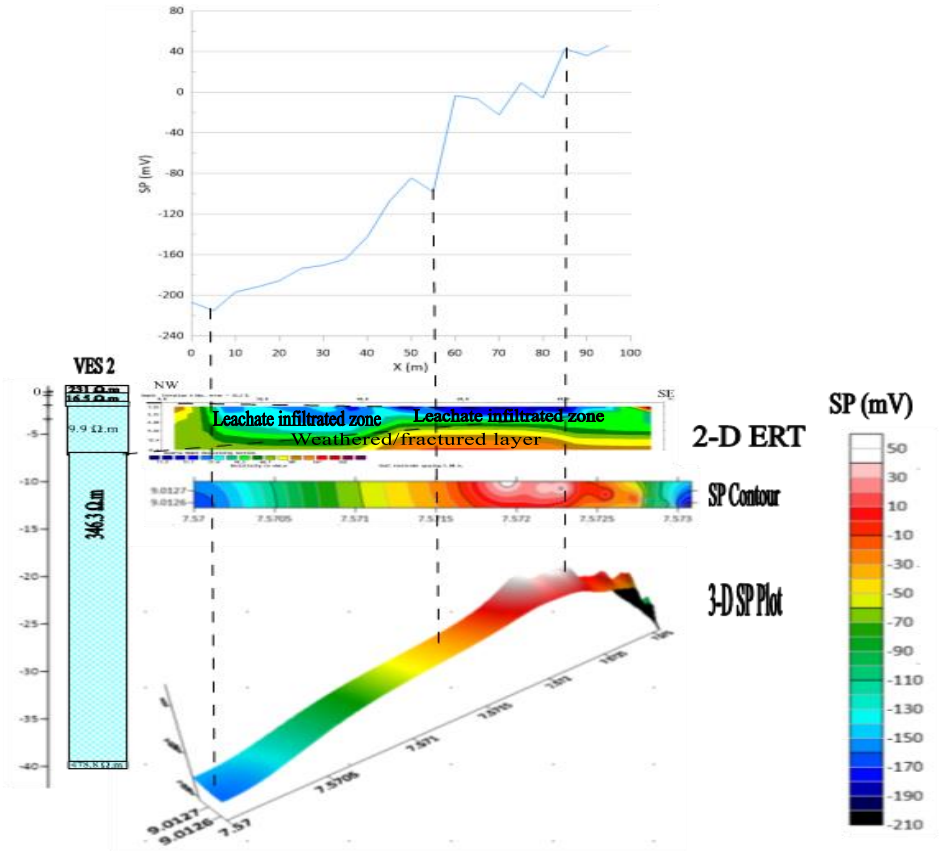

Figure 22: Cross-section correlating the SP profile, SP contours and 3-D SP plot and VES log along Profile 2 (Karu-Abuja)

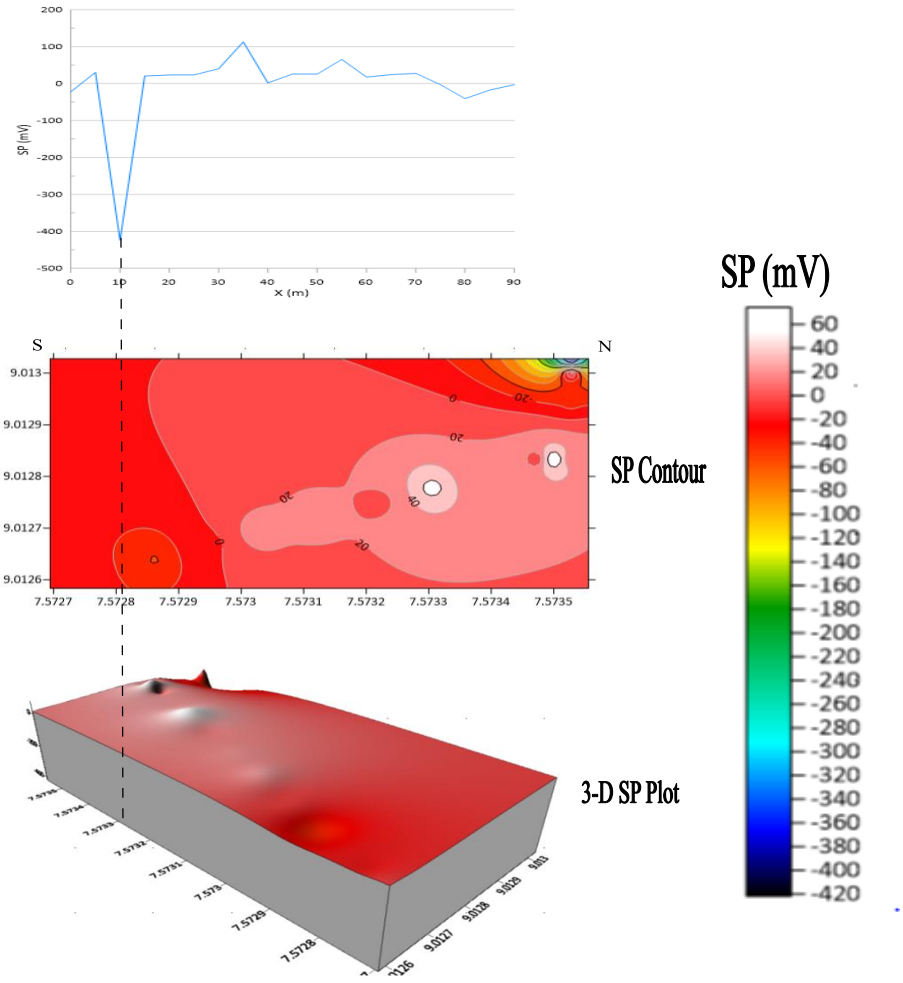

Figure 23: Cross-section correlating the SP profile, SP contours and 3-D SP plot and VES log along Profile 3 (Karu-Abuja)

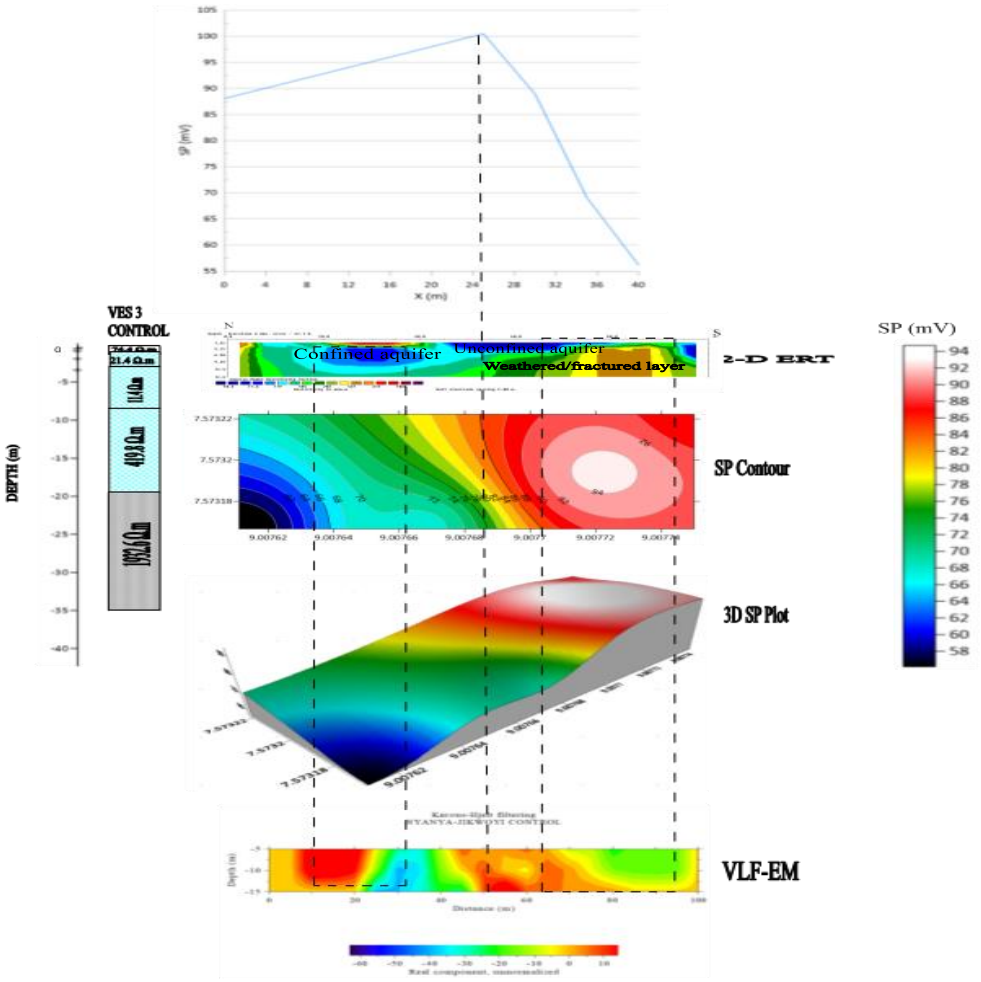

Figure 24: Cross-section correlating the SP profile, SP contours and 3-D SP plot and VES log along Profile 4 (Karu-Abuja Centre Centre)

3.5 Interpretation of Very Low Frequency Electromagnetic (VLF-EM) results

The results for the sixteen (16) VLF-EM Transverses created adjacent the Keffi and Karu-Abuja study areas indicating the fraser filtered, measured VLF and K-H pseudo cross-sections along transverses are shown in Figures 25 to 40:

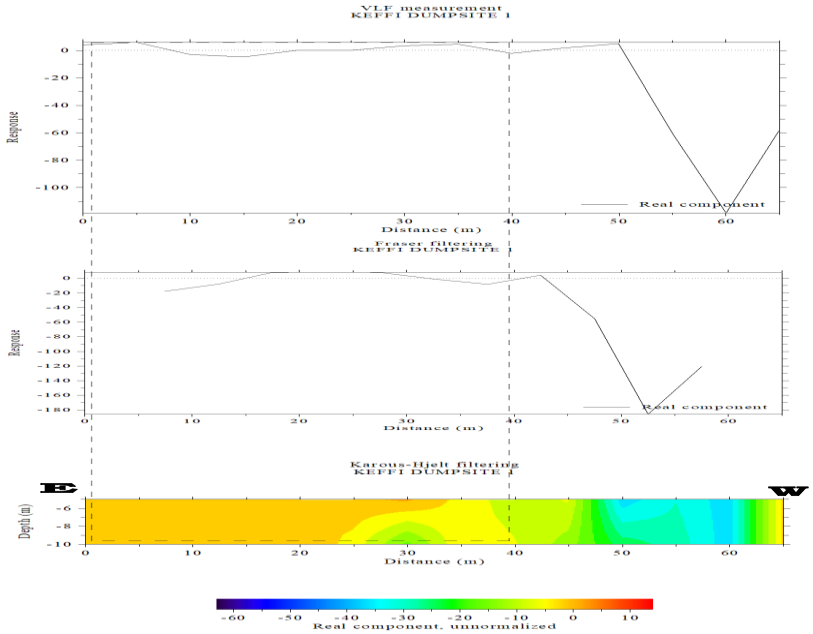

Figure 25: Cross-section of Fraser Filtered, measured VLF and K-H pseudo section along Transverse 1(Keffi)

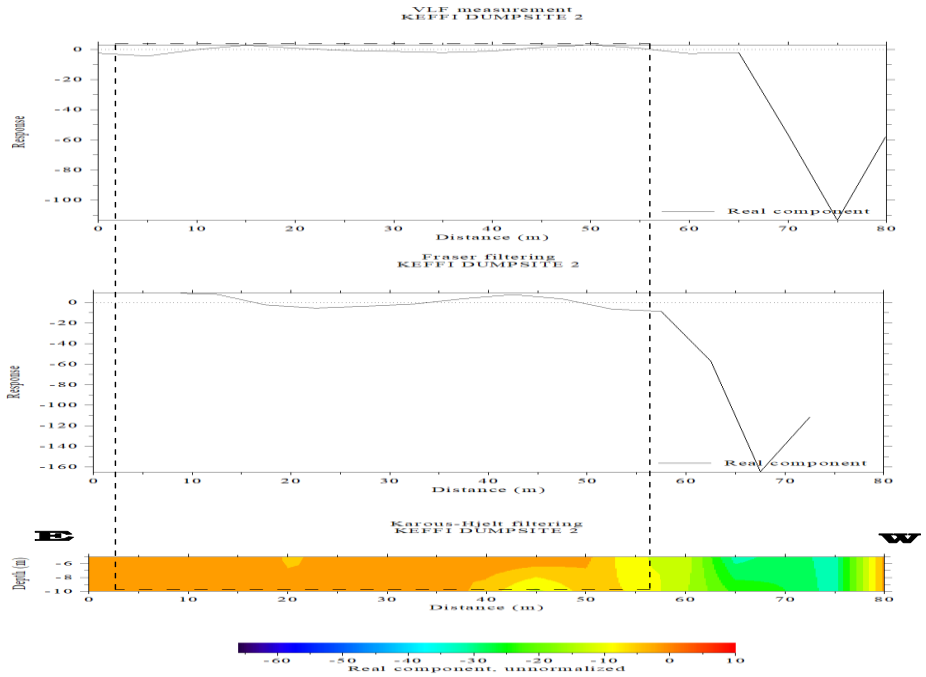

Figure 26: Cross-section of Fraser Filtered, measured VLF and K-H pseudo section along Transverse 2 (Keffi)

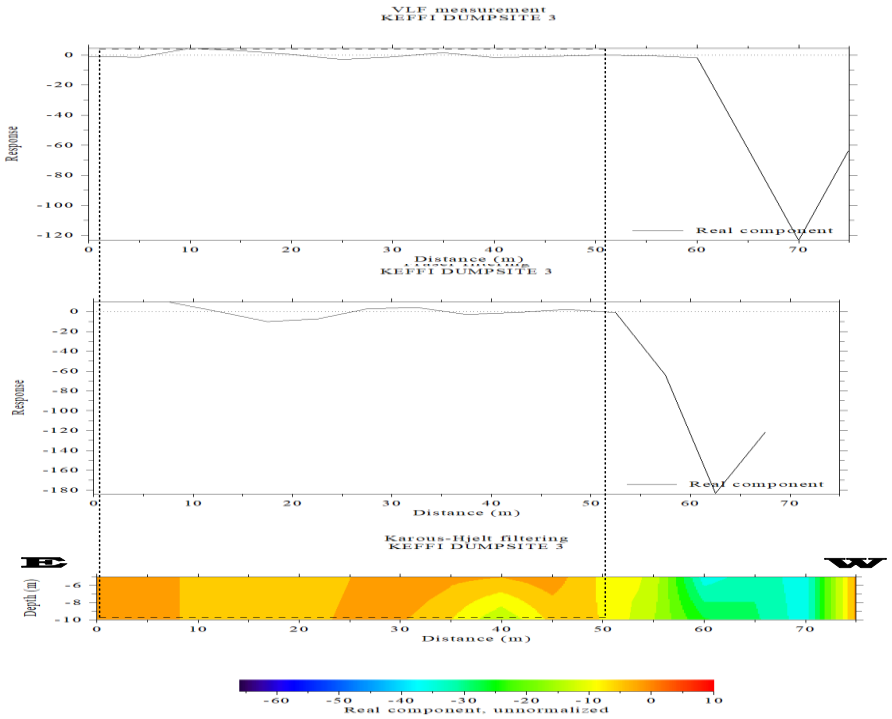

Figure 27: Cross-section of Fraser Filtered, measured VLF and K-H pseudo section along Transverse 3 (Keffi)

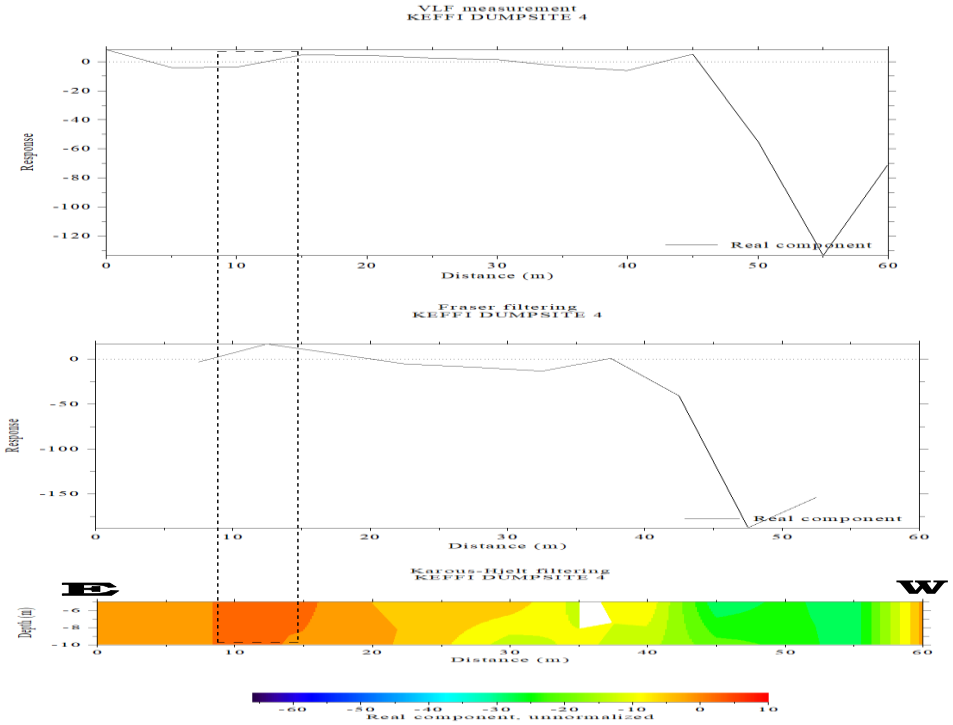

Figure 28: Cross-section of Fraser Filtered, measured VLF and K-H pseudo section along Transverse 4 (Keffi)

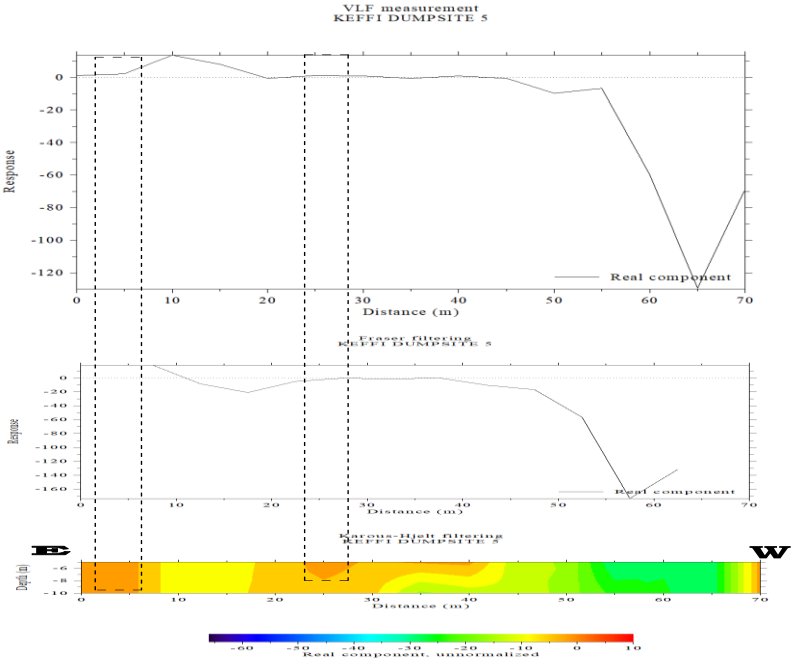

Figure 29: Cross-section of Fraser Filtered, measured VLF and K-H pseudo section along Transverse 5 (Keffi)

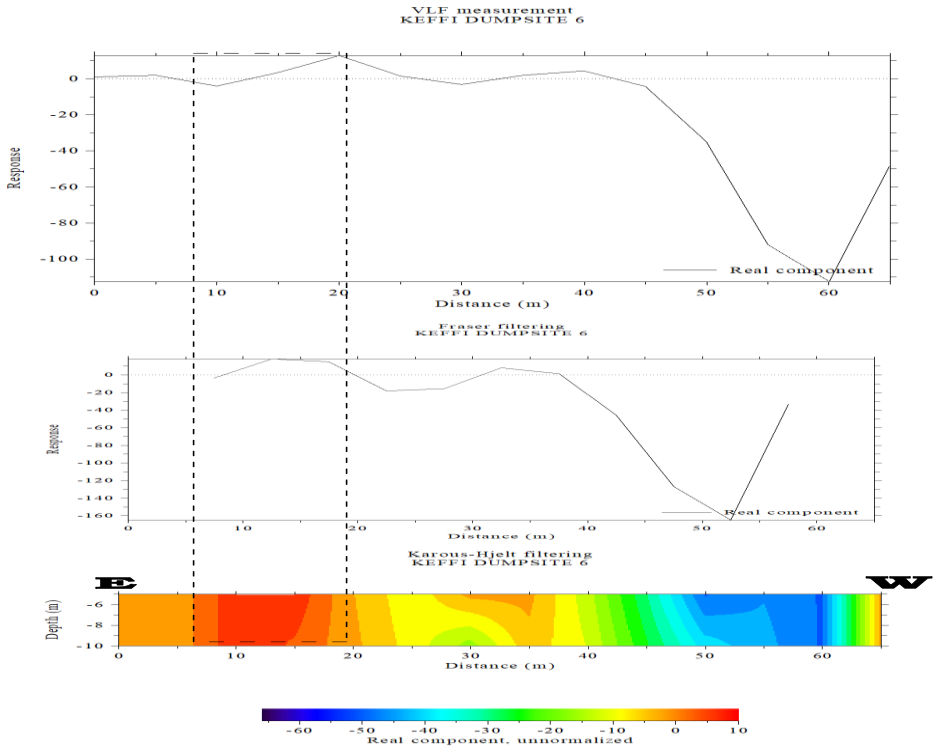

Figure 30: Cross-section of Fraser Filtered, measured VLF and K-H pseudo section along Transverse 6 (Keffi)

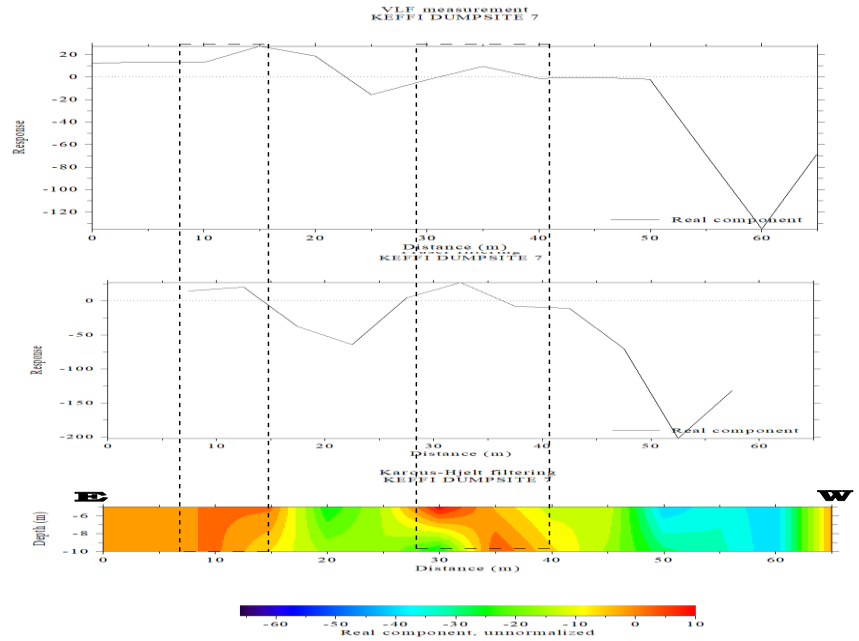

Figure 31: Cross-section of Fraser Filtered, measured VLF and K-H pseudo section along Transverse 7 (Keffi)

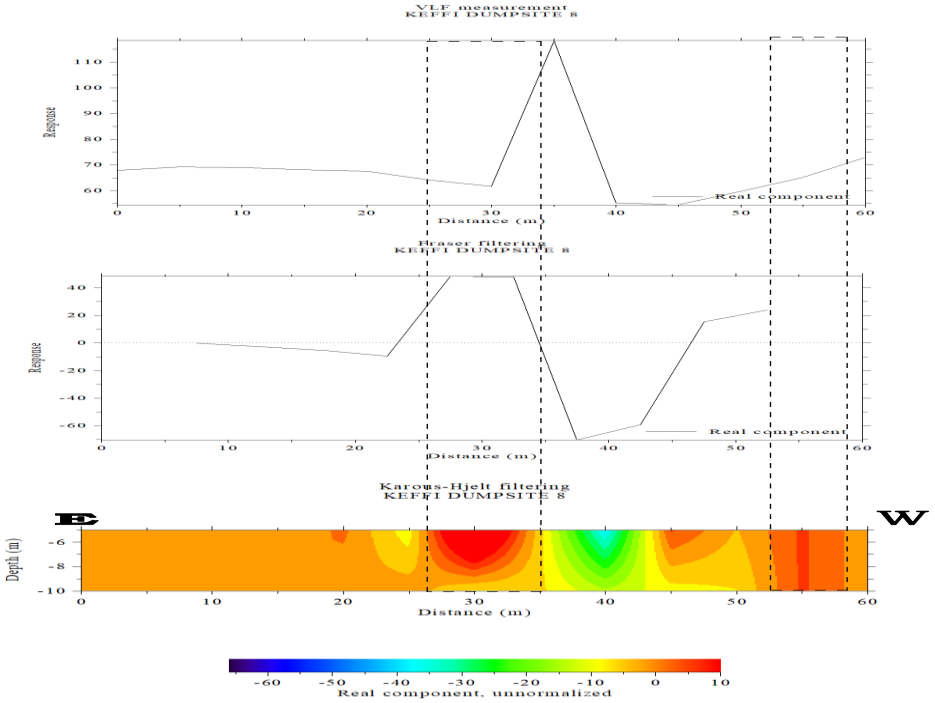

Figure 32: Cross-section of Fraser Filtered, measured VLF and K-H pseudo section along Transverse 8 (Keffi)

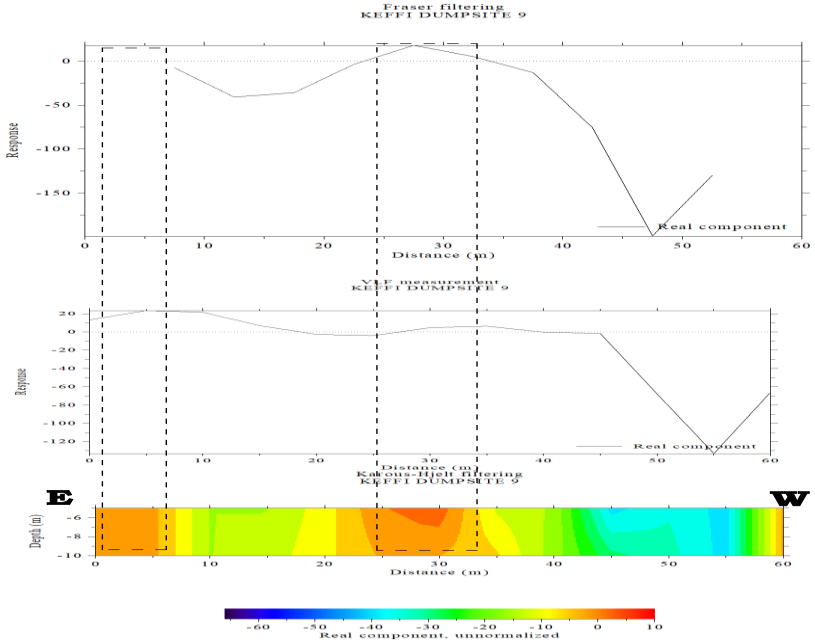

Figure 33: Cross-section of Fraser Filtered, measured VLF and K-H pseudo section along Transverse 9 (Keffi)

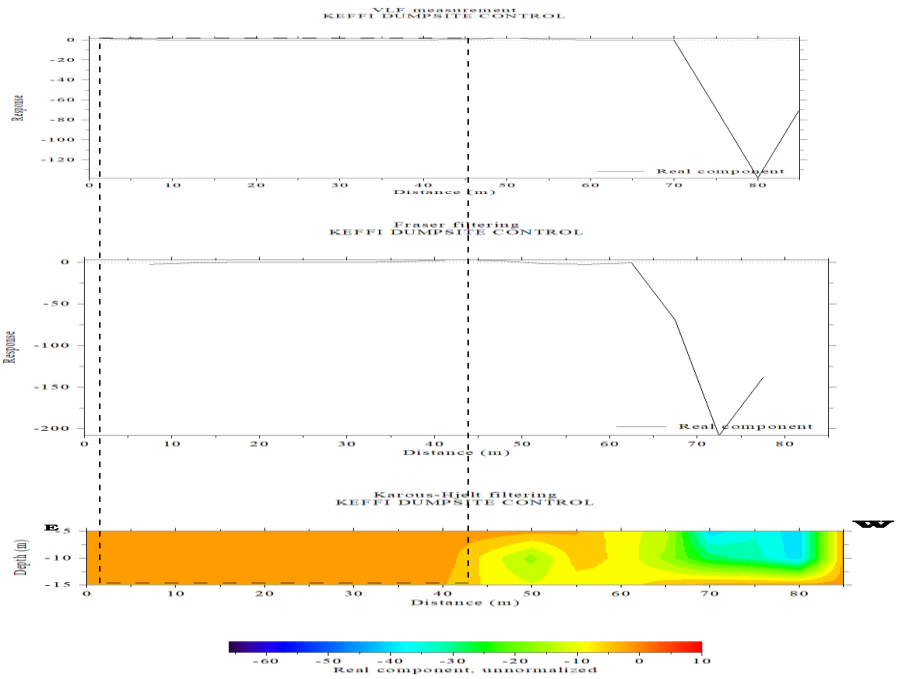

Figure 34: Cross-section of Fraser Filtered, measured VLF and K-H pseudo section along 10 (Keffi Control Centre)

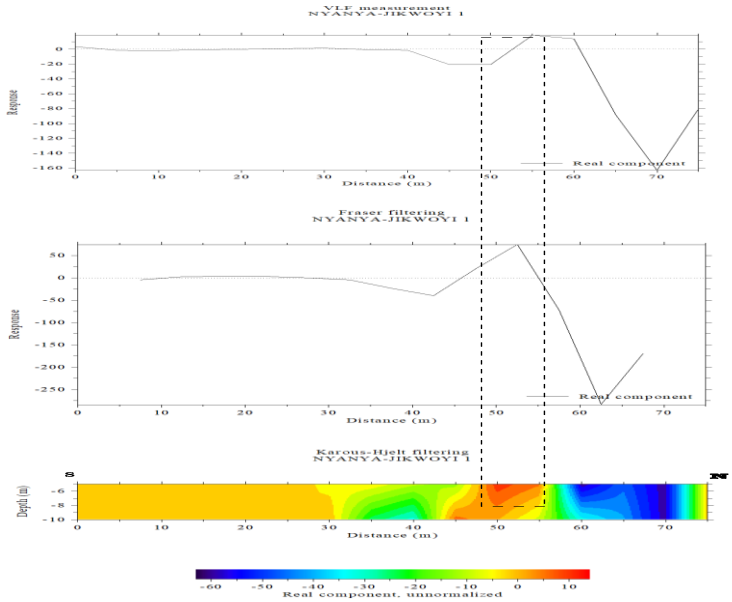

Figure 35: Cross-section of Fraser Filtered, measured VLF and K-H pseudo section along Transverse 1 (Karu-Abuja)

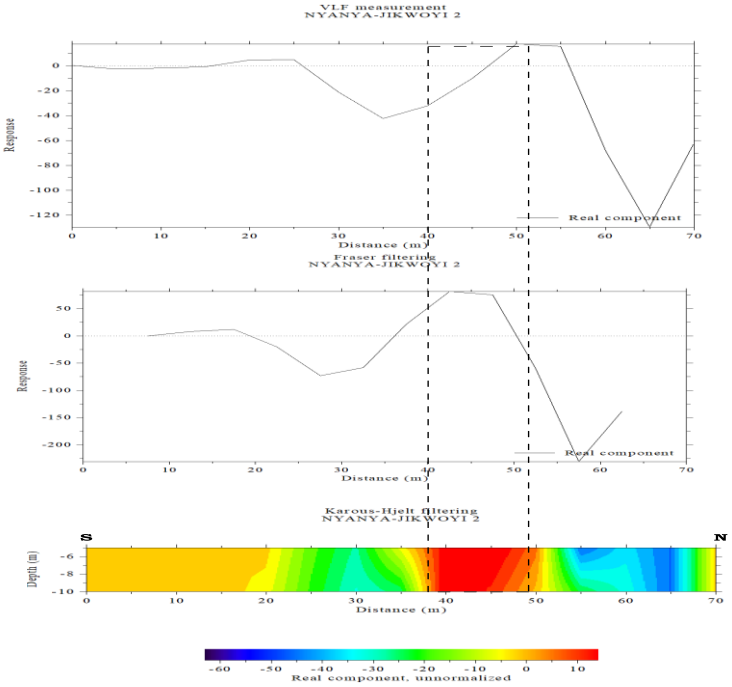

Figure 36: Cross-section of Fraser Filtered, measured VLF and K-H pseudo section along Transverse 2 (Karu-Abuja)

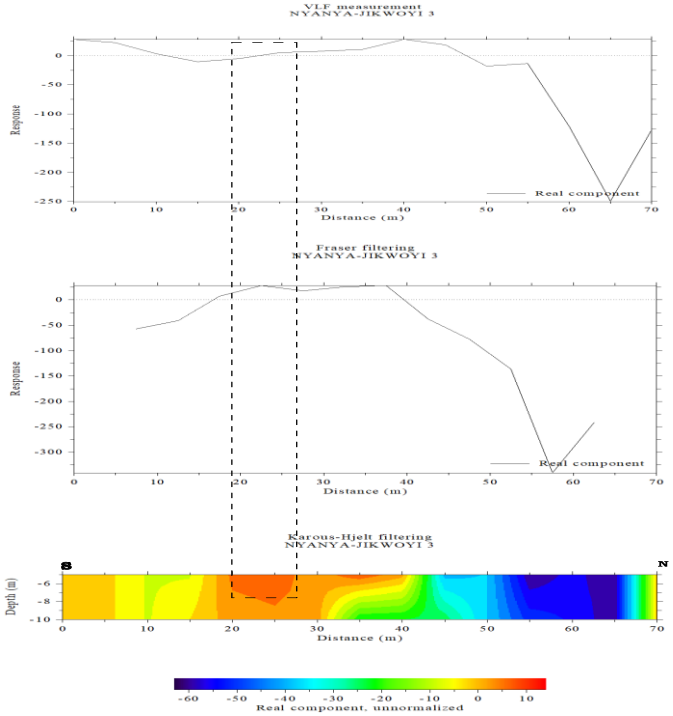

Figure 37: Cross-section of Fraser Filtered, measured VLF and K-H pseudo section along Transverse 3 (Karu-Abuja)

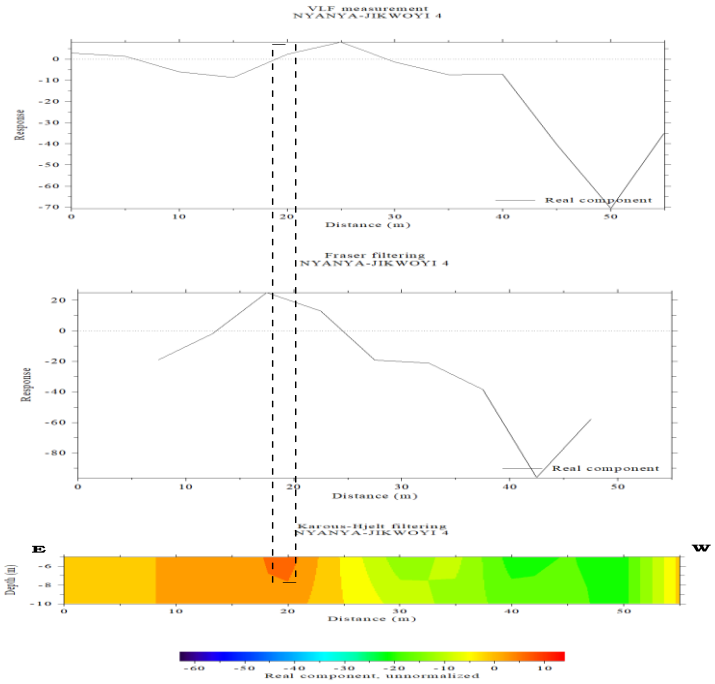

Figure 38: Cross-section of Fraser Filtered, measured VLF and K-H pseudo section along Transverse 4 (Karu-Abuja)

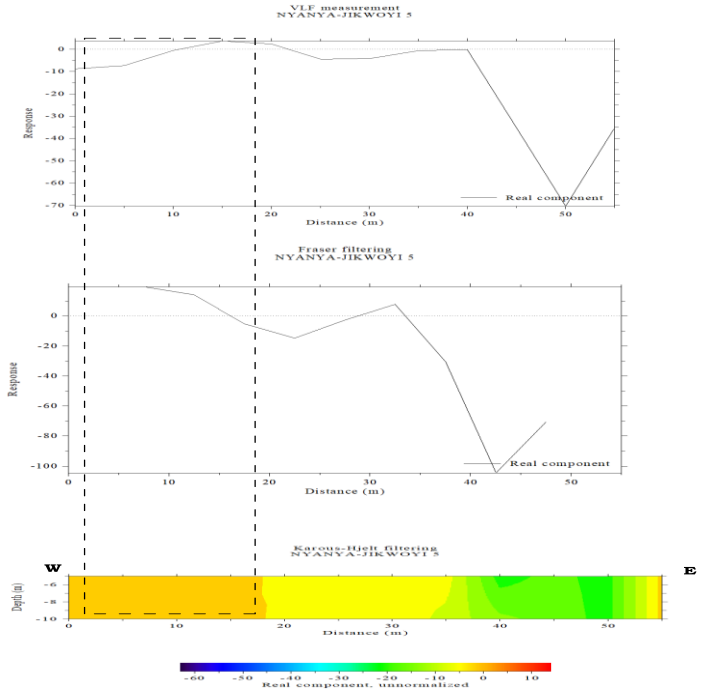

Figure 39: Cross-section of Fraser Filtered, measured VLF and K-H pseudo section along Transverse 5 (Karu-Abuja)

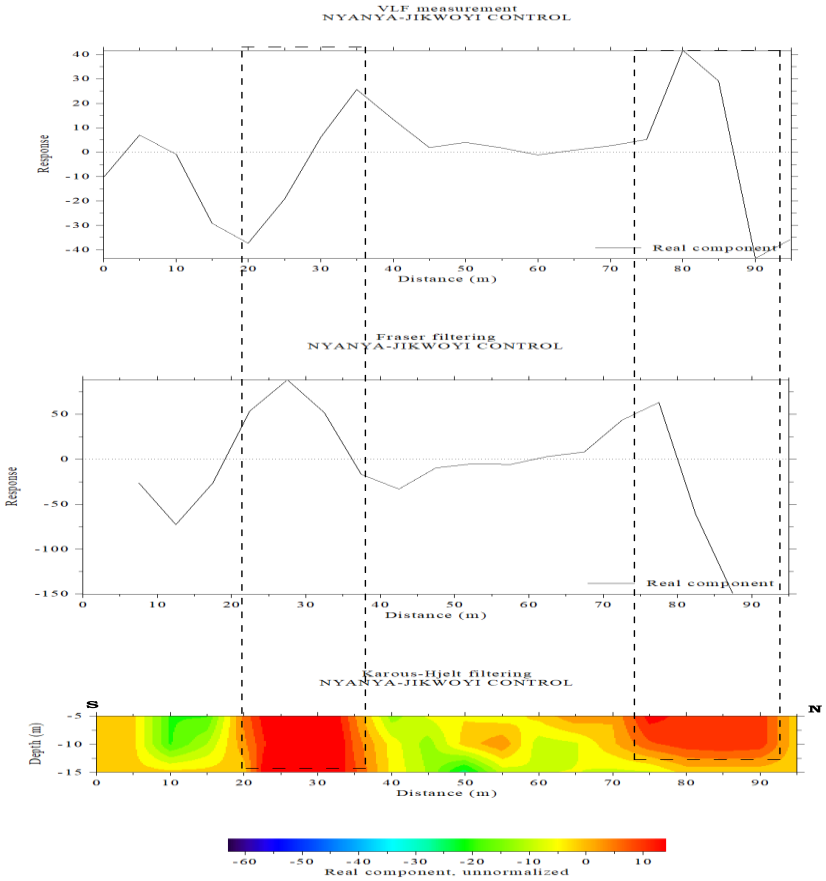

Figure 40: Cross-section of Fraser Filtered, measured VLF and K-H pseudo section along Transverse 6 (Control Centre, Karu-Abuja)

3.6 Discussion

The Keffi and Karu-Abuja study areas are characterised by heterogeneous lithology with resistivity values varying from low to high as displayed in the corresponding resistivity-depth profiles in Figures 4 to 12. The geo-electric sections revealed four to five discrete geo-electric layers, consisting of Topsoil (lateritic); second layer interpreted as weathered zone (clayey sand); the third layer inferred as fractured bedrock, while the fourth and fifth layers were interpreted as fresh bedrocks. The identified curve types from the model for the Keffi study area include: HA (50%), HK (33.3%), QA (16.7%). The HK type was identified at the Control Centre, while the identified curves for Karu-Abuja include: HA (33.3%), KHA (33.3%), and type QA (33.3%), identified at the Control Centre.

The Topsoil

The resistivity values for topsoil layers and their corresponding thicknesses for the Keffi study areas varies from VES 1 (47.1 to 9.6 Ω m), (0.5 to 4.1 m), VES 2 (199.5 to 12.8 Ω m), (1.1 to 1.7 m), VES 3 (224.2 to 66.8 Ω m), (0.8 to 19.5 m) VES 4 (113.5 to 18.9 Ω m), (2.1 to 6.2 m) VES 5 (230.6 to 78.1 Ω.m), (1.6 to 26.1 m) and VES 6 (Control Centre) (125.0 to 9.2 Ω m), (1.6 to 2.6), while that of Karu-Abuja varies from VES 1 (294.0 to 21.5 Ω.m), (0.6 to 0.4 m), VES 2 (16.5 to 231.2 Ω.m), (0.5 to 0.9 m), VES 3 (74.4 to 21.4 Ω.m), (0.7 to 2.2 m). This is suggestive of three zones: the belt of the soil water at the top, the intermediate vadose zone, and the capillary fringe at the bottom which acts as the passage for the flow of surface water to the fractured layer known as the zone of aeration.

The Second layer

The resistivity values for the second layers and their corresponding thicknesses for the Keffi study areas varies from VES 1 (9.6 to 116.4 Ω.m), (4.1 to 5.0 m); VES 2 (12.8 to 2.8 Ω m), (0.6 to 2.5); VES 3 (66.8 to 1,043.9 Ω.m), (19.5 to 16.7 m); VES 4 (18.9 to 3371.3 Ω.m), (6.2 to 19.7 m); VES 5 (78.1 to 364.9 Ω.m), (26.1 to 18.0 m) and VES 6 (9.2 to 195.9 Ω.m), (2.6 to 3.5 m), while that of Karu-Abuja varies from VES 1 (21.5 to 7.2 Ω.m), (0.4 to 1.0 m), VES 2 (231.2 to 131.8 Ω.m), (0.9 to 0.7 m), VES 3 (21.4 to 11.4 Ω.m), (2.2 to 5.8 m). This layer is mostly composed of weathered to fractured basement, clay, and limestone, in agreement with the geology of the area and consists of priority targets for groundwater exploration.

The third layer

Resistivity values for the third layers and their corresponding thicknesses for Keffi study areas varies from VES 1 (116.4 to 3061.4 Ω.m), (5.0 to 42.8 m), VES 2 (2.8 to 1257.6 Ω.m), (2.5 to 19.2 m), VES 3 (1043.9 to 6696.0 Ω.m), (16.7 to infinity), VES 4 (3,371.3 to 13,402.7 Ω.m), (19.7 to infinity), VES 5 (364.9 to 2,985 Ω.m), (18.0 m to infinity), VES 6 (5,384.7 to 9,152.0 Ω.m), (35.0 m to infinity), while that of Karu-Abuja varies from VES 1 (7.2 to 221.7 Ω.m), (1.0 to 1.4 m), VES 2 (131.8 to 9.9 Ω.m), (0.7 to 0.7 m), VES 3 (11.4 to 419.8 Ω.m), (5.8 to 12.1 m). This layer is mostly composed of fractured bedrock and consolidated sandstones. The fourth layer for Karu-Abuja consists of materials with resistivity values which varies from VES 1 (221.7 to 57,293.9 Ω.m), (1.4 m to infinity), VES 2 (9.9 to 346.3 Ω.m), (5.5 to 35.2 m), VES 3 (419.8 to 1,932.6 Ω.m), (12.1 m to infinity). This layer is composed of fractured to fresh basement, while the fifth/sixth layer for the Karu-Abuja study area comprises materials with resistivity values which varies from VES 1 (57, 293.9 Ω.m to infinity), (1.4 m to infinity), VES 2 (346.3 to 478.8 Ω.m), (35.2 m to infinity), VES 3 (1,932.6 Ω.m to infinity). This layer is mostly composed of fresh basement.

3.7 Estimated Aquifer Protective Capacity (APC) for the study area (Karu-Abuja)

The calculated Longitudinal Conductance S (Table 3) for the Keffi study area revealed that the aquifer protective capacity is rated as poor to good with four VES points (VES 1 (0.043 S), VES 4 (0.05 S), VES 5 (0.01 S) and VES 6 (0.02 S)) representing 66% of the sounding points, indicating poor protective capacity rating; two VES points (VES 3 (0.29 S) and VES 4 (0.33 S)) representing 33.33% of the soundings, showed moderate protective capacity rating, while only

VES 2 (0.89), representing 16.6% of the soundings, showed good protective capacity. The aquifer protective rating of VES points indicating poor protective capacity (66 %). However, the calculated Longitudinal Conductance S (Table 5) for the Karu-Abuja study area revealed that the aquifer protective capacity ranged from poor to weak; with the combined VES points VES 1 (0.0063 S) and VES 3 (0.002 S), representing 66.6% of the sounding points, indicating poor protective capacity; while VES point VES 2 (0.1 S) representing 33.3% of the soundings, shows weak protective capacity. Although both results suggests that the study areas are not suitable for the establishment of landfills, attributed to insufficient impervious clay seals to protect groundwater resources from leachate infiltration, Keffi is preferable to the Karu-Abuja study area.

3.8 Delineation of aquifer systems

Two borehole logs (after Anudu *et al*. 2021) obtained from a distance of about 50 m from the Keffi study area were used to correlate with VES points along the profiles. Borehole log (BH D) was used to infer the lithologic sections derived from the interpretations of VES profiles (1 to 5) around the dumpsite, while Borehole log (BH C) was used to correlate the VES point for the control centre (Fig. 13), while, a borehole log (BH) (after Sunkari *et al.*2021) was used to correlate with VES points along the profiles and used to infer the lithologic sections derived from the interpretations of VES profiles (1 to 3) around the dumpsite and the Control Centre with a view to delineating the aquifer systems in the area (Fig. 14). The results correlated well with each layer.

3.8.1 CORRELATION ANALYSIS

The following sections correlates the Self Potential (mV) profiles, their corresponding SP contours and 3-D SP plots, VES transverses and 2-D ERT geo-electric sections along the survey lines (Figures 15 – 24):

3.9 Profile 1 (Keffi)

The SP anomalies along profile 1 (Figure 15) indicate dominant negative SP distribution patterns ranging from (-100 to -5 mV) between (0 – 120 m) along the survey line. Between (0 to 10 m) is a sharp deviation of the SP anomaly ranging from (-80 to -60 mV) attributed to leachate induced electro-kinetic process flowing in the S-N direction. This correlates with the VES results indicating the presence of materials with low resistivity value of (9.6 Ω.m, in depths ≥ 10 m) along the same transverse, suggestive of leachate infiltrated zone.

3.10 Profile 2 (Keffi)

This cross-section (Figure 16) correlates the 2-D ERT, SP contours, 3-D SP plot and SP (in mV) profile 2. The 2-D ERT delineated three (3) geo-electric sections. Stretching from the eastern to the western flank are materials with resistivity values ranging from (53 to 412 Ω.m, in depths ≥ 3.73 m). This was inferred as the topsoil. From the eastern flank, are objects with resistivity values ranging from (6.83 to 19.3 Ω.m, in depths ≥ 6.38 m), along (0 to 20 m) interpreted as leachate contaminants flowing in the E-W direction. This result was correlated by the VES log showing objects with low resistivity materials ranging from (2.8 to 12.8 Ω.m, in depths ≥ 8.5 m). Situated between (50 to 70 m) at the central part of the profile, is a protruded conic-shaped object

with resistivity values ranging from (6.83 to 10 Ω.m). This was also interpreted as leachate plume intrusion. At the western flank, spanning between (70 to 90 m) along the survey line, are materials with resistivity values ranging from (53 to 412 Ω.m) interpreted as weathered/fractured bedrock. Between (90 to 120 m) are materials with resistivity values ranging from (1147 to 8996 Ω.m, in depths ≥ 9.26 m) are materials interpreted as fresh basement. This result is correlated by the presence of materials with negative SP anomalies ranging from (- 50 to -10 mV), situated between (10 – 16 m) along the survey line, suggestive of leachate infiltrated contaminants. The 3-D SP contour map also depicts the E-W direction of leachate flow which is closely related to the topographic conditions of the study area. The positive SP anomalies are interpreted as quartz veins in agreement with the geology of the area.

3.10.1 Profile 3 (Keffi)

This cross-section (Figure 17) compares the VES Log, SP contours and 3-D SP plot for profile 3. The dominant materials with negative SP values ranging from (-90 to -5 mV) located between (0 – 160 m) along the survey line, is attributed to groundwater streaming potential. This was correlated with the VES results which shows presence of materials with higher resistivity values ranging from (66.8 to 224.2 Ω.m, in depths ≥ 20 m), along the survey line, suggestive of saturated fractured zone. The absence of materials with low resistivity values along the survey line established that the zone is free from leachate contamination due to the distance of the transverse which is 150 m away from the dumpsite.

3.10.2 Profile 4 (Keffi)

This cross-section (Figure 18) compares the VES Log, SP profile, SP contours and 3-D SP plot for profile 4. The SP values indicate a variation of positive and negative SP distribution patterns ranging from (-50 to 70 mV) between (0 – 140 m). This is attributed to fluid streaming potential. The VES results with resistivity values ranging from (18.8 to 113.5 Ω.m, in depths ≥ 20 m) are diagnosed as aquifer material hosting groundwater resources. The survey line's distance from the dumpsite, which is 250 meters, indicates that the low resistivity values are not due to the presence of leachate contaminants.

3.10.3 Profile 5 (Keffi)

This cross-section (Figure 19) compares the VES Log, SP profile, SP contours and 3-D SP plot for profile 5. The contour map of the self-potential showing variation of positive and negative values ranging from (-200 to 450 mV) is attributed to streaming potential. This was correlated by VES results showing materials with resistivity values ranging from (78.1 to 364.7 Ω.m, in depths ≥ 46 m). The streaming potential is attributed to groundwater flow, as against leachate as an electrical conductivity source, given the survey line's distance (about 300 m away) from the dumpsite.

3.10.4 Profile 6 (Control Centre, Keffi)

This cross-section (Figure 20) correlates the VES log, 2-D ERT, SP profile, SP Contour and 3-D SP plot along profile 6 (Control Centre). The materials with low resistivity values ranging from (32.6 to 71.2 Ω.m, in depths ≥ 12.4 m), stretching from (40 to 120 m), was interpreted as unconfined aquifer material. From the southern flank are materials with resistivity values ranging from (348 to 582 Ω.m, in depths ≥ 15.9 m), suggestive of fractured layer. Also inferred as

fractured zone are objects with resistivity values ranging from (156 to 582 Ω.m, in depths ≥ 15.9 m) situated between (40 to 120 m). Comparatively, the resistivity values of (6.83 Ω.m) recorded near the dumpsite was lower than 32.8 Ω.m, recorded at the Control Centre. This established the presence of leachate contaminants near the dumpsite. The positive and negative variation of SP values ranging from (-90 to 120 mV) along the profile is attributed to groundwater streaming potential, while the materials with resistivity values ranging from (348 - 582 Ω.m, in depths ≥ 9.25 m),) located between (5 to 10 m), is diagnosed as fractured layer with potential for groundwater exploration.

3.11 Profile 1 (Karu-Abuja)

This cross-section (Figure 21) correlates the SP profiles, SP contours, 3-D SP and VES Log. The SP profile shows positive SP anomalies ranging from (160 to 360 mV) between (0 – 90 m) diagnosed as streaming potentials attributed to an adjourning stream and leachate flow in the E–W direction. This was correlated by materials with low resistivity value of (7.2 Ω.m, in depths ≥ 2.0 m) from the VES log interpreted as leachate plume.

3.12 Profile 2 (Karu-Abuja)

This cross-section (Figure 22) correlates the SP profile, 2-D ERT, SP contours and 3-D SP plot for profile 2.The 2-D ERT geo-electric section identified three layers. The topsoil (consist of laterite soil and leachate infiltrated zones); the weathered and the fractured basement. The materials with low resistivity values ranging from (11.3 to 15.9 Ω.m, in depths ≥ 6.63 m) spread between (0 – 100 m) suggests leachate infiltrated zone flowing in the NW - SE direction. From the NW flank, is a material with resistivity value ranging from (27.8 to 66.8 Ω.m, in depths ≥ 12.4 m) situated between (0 to 40 m) interpreted as weathered layer. Between (50 to 100 m) are materials with resistivity values ranging from (187 to 262 Ω.m), interpreted as deep seated fracture acting as water conduits to the vadose zone. The proximity of a protruding material in the southeastern axis, interpreted as leachate plume, suggests that groundwater resources in the area must have been contaminated by leachate. The dominant negative SP anomalies ranging from (-210 to -1 mV) along the survey line, which increased exponentially at the central point, were similarly correlated as leachate accumulation. The positive SP anomalies beyond (60 m to 100 m) were diagnosed as bioelectric materials emanating from decomposing corpses from a cemetery adjacent the study area. The 2-D ERT and SP results were correlated by the VES geo-electric section along the survey line which revealed the presence of low resistivity materials ranging from (9.9 to 16.5 Ω.m, in depths ≥ 7.7 m) suggestive of leachate infiltrated zone.

3.13 Profile 3 (Karu-Abuja)

This cross-section (Figure 23) compares the SP profile, SP contour and 3-D SP plots for profile 3. The dominant negative SP anomaly ranging from (-420 to -20 mV) which peaked between (0 – 10 m) is attributed to redox reaction influenced by deep seated leachate accumulation. Further away from the dumpsite, between (20 to 90 m) was rebound with a positive SP anomaly ranging from (0 to 60 mV). This was interpreted as streaming potentials.

3.13.1 Profile 4 (Control Centre, Karu-Abuja)

This cross-section (Figure 24) correlates the SP profile, the 2-D ERT, SP contours, 3-D SP plot and VES log for the Control Centre. The low resistivity materials from the northern flank, ranging from (50.4 to 77.6 Ω.m, in depths ≥ 12.4 m) situated beneath a suspected clay seal between (20 to 40 m) is interpreted as a confined aquifer with groundwater potential. On the

southern flank is a material with resistivity values ranging from (50.5 to 60 Ω.m, in depths ≥ 6.3 m)situated between (40 to 80 m), diagnosed as an unconfined aquifer. Between (0 to 50 m) are materials with resistivity values ranging from (119 to 283 Ω.m, in depths ≥ 15.9 m). This is interpreted as a weathered layer. Materials with resistivity values ranging from (438 to 673 Ω.m, in depths ≥15.9 m) located on the northern flank; between (60 to 100 m), is suggestive of a fractured basement. This was correlated by VES log showing materials with resistivity values ranging from (11.4 to 419.8 Ω.m, in depths ≥ 8.7 m) along the transverse. The dominant positive SP anomalies ranging from (58 to 94 mV) along the survey line, suggests the presence of geochemical reactions attributed to groundwater flow in the S-N direction. The VLF-EM similarly shows material with positive current-density ranging from (5 to 10 %) situated along (10 to 20 m and 40 to 70 m, in depths ≥ 15 m) along the survey line. This is suggestive of weathered/fractured materials hosting groundwater resources.

3.13.2 Analysis of the VLF-EM Profiles

VLF-EM profiles 1 - 6 were established along the Keffi study area and shows places of high positive current-density anomaly ranging from (-10 to 10%) and covering (0 to 40 m) to depths of 10 m. This indicates lateral and vertical spread of leachate from the eastern to western part of the dumpsite into the subsurface. The areas with high negative anomaly ranging from (-20 to -60 %, in depths ≥ 14.5 m) covering (40 to 65 m) are interpreted as crystalline rocks with low conductivity. The strength of the positive anomaly, as reflected along profile 8, decreased as the profile distance from the dumpsite increased. The vicinity around 40 m – 65 m along profiles 1, 2, and 3 also show high positive anomaly that decreased in magnitude and size with distance from the Centre of the dumpsite. At profile 6, low positive current density indicates the absence of leachate at shallow subsurface. Places showing high positive current density are interpreted as soil and rocks infiltrated by leachate. The two VLF-EM profiles established outside the dumpsite show lower current density (profiles 5, 6, 7, 8) than profiles established closer to the dumpsite (profiles 1, 2 and 3). This suggests that high current density is due to the presence of leachate. Along the Control Centre (Transverse 10), between (0 to 40 m) are materials with high positive current-density anomaly ranging from (0 to 5%, in depths ≥ 15 m), suggestive of groundwater saturated zones. In the western flank, are objects with high negative anomaly ranging from (-15 to -40 %, in depths ≥ 15 m) between (45 to 85 m), interpreted as low conductivity rocks.

Six (6) VLF-EM profiles were established along the Karu-Abuja study areas and revealed the following:

3.13.3 Transverse 1

From the starting point of (Figure 35) along the survey line, between (0 to 30 m) are yellowish materials with current density ranging from (-5 to 5 %, in depths ≥ 15 m) suggestive of conductive materials flowing in the S – N direction. Between (40 to 51 m) along the profile are reddish prominent materials with high positive anomaly ranging from (5 to 10%, in depths ≥ 10 m). This is suggestive of leachate generated electrical conducting paths. Between (30 to 42 m) are greenish materials with negative anomaly ranging from (-10 to -25 %) suggestive of rock intrusions. Between (60 to 80 m) are bluish materials with negative current density (-10 to -60 %) suggestive of fractured bedrock.

3.13.4 Transverse 2

From the starting point (0 to 20 m) along the survey line (Figure 36) are yellowish materials with current density ranging from (-5 to 5 %) suggestive of conductive materials flowing in the S – N direction. However, between (40 to 51 m) along the profile are reddish materials with prominent high positive anomaly ranging from (5 to 10%) along the survey line. This is suggestive of lateral and vertical spread of leachate into the subsurface. Between (20 to 37 m) are greenish materials with negative anomalies ranging from (-10 to -25 %) suggestive of intercalations of clay and sandstones. Between (51 to 70 m) are bluish and greenish materials with negative current-densities ranging from (-10 to -60 %) suggestive of fractured bedrock.

3.13.5 Transverse 3

From the starting point (0 to 20 m) along the survey line (Figure 37) are yellowish and greenish materials with current density ranging from (-20 to 1 %) suggestive of conductive materials flowing in the S – N direction. However, between (20 to 30 m) along the profile are materials with prominent high positive anomaly ranging from (5 to 11 %) along the survey line. This is suggestive of leachate generated electrical conducting paths. Between (30 to 50 m) are greenish materials with negative anomalies ranging from (-20 to -30 %) suggestive of hardpan. At distances between (50 to 70 m) are deep bluish and greenish materials with negative current densities ranging from (-10 to -65 %) suggestive of fractured bedrock.

3.13.6 Transverse 4

The material (Figure 38) with high positive anomaly ranging from (5 to 10%) between (10 to 25 m) is suggestive of lateral and vertical spread of leachate flowing in the E – W direction. Between (0 to 10 m) is yellowish material with high negative and positive current densities anomaly ranging from (-5 to -5 %, in depths ≥ 10 m) suggestive of lateritic soil. Between (25 to 60 m), are intercalations of greenish and lemon materials suggestive of lineament structures.

3.13.7 Transverse 5

Starting from (0 to 10 m) (Figure 39) are yellowish materials with negative and positive current density anomaly ranging from (-5 to 5 %) suggestive of leachate infiltrated zones flowing in the W – E direction. Between (20 to 35 m) are yellowish materials suggestive of lineament structures. Between (35 to 60 m) are patches of greenish and yellowish materials with current density ranging from (-20 to -5 %) suggestive of mineralized pegmatite which outcrops the study area.

3.13.8 Transverse 6 (Control Centre, Karu-Abuja)

Transverse 6 (Figure 40) is the Control Centre situated approximately 500 m away from the dumpsite. The results revealed that materials with prominent positive current-density ranging from (5 to 10 %) situated along (10 to 20 m and 40 to 70 m, in depths ≥ 15 m) are suggestive of weathered/fractured materials hosting groundwater resources. Between (20 to 40 m) and (80 to 100 m) are blue, green and yellow patches suggestive of mineralised intrusions.

3.14 Evaluation of the conductive layers

Materials with resistivity values (≥ 6.83 Ω.m) were delineated as leachate infiltrated and soil-contaminated zones in both areas. The occured along transverse 2 and in parts of transverse 1, at maximum depth of 9.26 m and at an average depth of 6.38 m in the Keffi study area, and along transverses 1 and 2, at maximum depth of 5.5 m at an average depth of 3.25 m in the Karu-Abuja study areas. The low resistivity values, negative SP anomalies and prominent high current-density anomalies observed at the Keffi Control Centre is attributed to a stream situated adjacent the Control Centre — which recharges its aquifer. The low resistivity and positive current-density anomalies observed at the Karu-Abuja Control Centre is attributed to presence of a confined aquifer — which is a priority target for high groundwater exploration. Comparatively, the resistivity values of leachate and negative SP anomalies detected around the dumpsites are lower than the values observed at the Control Centres.

4. Conclusion

The study used integrated geophysical methods to assess aquifer vulnerability in Karu-Abuja and Keffi, comparing the susceptibility of aquifer systems to leachate contamination. This involved the establishment of nine VES points using the Schlumberger array, four 2-D ERT profiles using the Wenner configurations, ten SP profiles, and sixteen VLF transverses near the dumpsites and the control areas. The Ohmega (Allied Geophysics) resistivity meter and Gem portable receiver systems were used to acquire the data, while interpretation of data employed tools such as WINRESIST, RES2DINV, GRAPHER, SURFER and KHFFILT. These methods identified groundwater saturation zones and contamination pathways, including fractures and faults. The resistivity values of the topsoil whichranges from (47.1 to 224.2 Ω.m) and (16.5 to 294.0 Ω.m) extending to depths ≥ 2.1 m and 0.5 m in Karu-Abuja and Keffi respectively, suggests that the overburden ofstudy areas are composed of low-permeable unconsolidated clay, sandy, and gravel materials. The estimated Aquifer Protective Capacity (APC) from the VES resistivity data, indicated poor to good rating for Keffi, and poor to weak for Karu-Abuja, which were validated by the borehole logs. Results revealed that Keffi has appreciably thicker overburden than the Karu-Abuja study areas and thus, better aquifer protective layers. Comparatively, the findings revealed that the Keffi study areas possess better impervious clay seals to protect groundwater resources against leachate infiltration than the Karu-Abuja. Regular Environmental Impact Assessments (EIAs) and the installation of geo-synthetic clay liners at the base of the dumpsites to safeguard groundwater resources from leachate infiltration are therefore recommended.

Authors' contributions

This work was carried out in collaboration among all authors. All authors read and approved the final manuscript.

Disclaimer (Artificial intelligence)

Option 1:

Author(s) hereby declare that NO generative AI technologies such as Large Language Models (ChatGPT, COPILOT, etc.) and text-to-image generators have been used during the writing or editing of this manuscript.

References

Abdel-Shafy, H. I., Ibrahim, A. M., Al-Sulaiman, A. M., & Okasha, R. A. (2024). Landfill leachate: Sources, nature, organic composition, and treatment: An environmental overview. *Ain Shams Engineering Journal*, *15*(1), 102293.

Ajibade, A. C., and Fitches, W. R. (1988). The Nigerian precambrian and the Pan-African orogeny. Precambrian geology of Nigeria, 1, 45-53.

Anudu, G.K., Obrike, S.E. and Ofoegbu, C.O. 2021 Groundwater Investigation Across the Crystalline Basement Rocks in Rogo Area, Kano State Northern Nigeria, Using Resistivity Methods (Keffi Borehole log).

Arowoogun, K. I., and Osinowo, O. O. (2022). 3D resistivity model of 1D vertical electrical sounding (VES) data for groundwater potential and aquifer protective capacity assessment: A case study. *Modeling Earth Systems and Environment,* 8(2), 2615-2626.

Arthur, J. C. (2024). Water Quality and Health Risk Assessment of Ground Water from Dump Site around Uguwaji Waste Dumpsite, Enugu Metropolis.

Bashir, M. Z. (2018). Geology of The Area Around Kurafe Hausawa, Part of Keffi Sheet 208 nw. 61.

Chinyem, F. I., & Ovwamuedo, G. (2024). Evaluation of aquifer characteristics and groundwater protective capacity in Abavo, Nigeria. International Journal of Geosciences, 15(11), 841-860.DOI: 10.4236/ijg.2024.1511046.

Chinyem, F.I. Determination of aquifer hydraulic parameters and groundwater protective capacity in parts of Nsukwa clan, Nigeria. *Environ Monit Assess* 196, 243 (2024). DOI: https://doi.org/10.1007/s10661-024-12411-w.

Dada, S. S. (2006). Proterozoic evolution of Nigeria. The basement complex of Nigeria and its mineral resources (A Tribute to Prof. MAO Rahaman). Akin Jinad and Co. Ibadan, 29-44.

de Groot S.R., and P. Mazur, Non-linear thermodynamics. *Dover Publications.* 1983. 510 p.

Ejepu, J. S., Jimoh, M. O., Abdullahi, S., Abdulfatai, I. A., Musa, S. T., & George, N. J. (2024). Geoelectric analysis for groundwater potential assessment and aquifer protection in a part of Shango, North-Central Nigeria. *Discover Water*, *4*(1), 33.

Koliyabandara, P. A., Preethika, D. D. P., Cooray, A. T., Liyanage, S. S., Siriwardana, C., & Vithanage, M. (2024). The Environmental Pressure by Open Dumpsites and Way Forward. In *Technical Landfills and Waste Management: Volume 1: Landfill Impacts, Characterization and Valorisation* (pp. 171-204). Cham: Springer Nature Switzerland.

McCurry, M. O. (1985). Petrology of the Woods Mountains volcanic center, San Bernardino County, California. California Univ., Los Angeles (USA).

Nataraj, S. K. (2024). *Materials and Methods for Industrial Wastewater and Groundwater Treatment*. John Wiley & Sons.

NGSA (Nigeria Geological Survey Agency) 2019. Geological map of Abuja. Published by the Authority of the Federal Republic of Nigeria.

Oladapo, M. I., and Akintorinwa, O. J. (2007). Hydrogeophysical study of ogbese south western Nigeria. *Global journal of pure and applied sciences*, 13(1), 55-61.

Oluwafemi, O., and Oladunjoye, M. A. (2013). Integration of surface electrical and electromagnetic prospecting methods for mapping overburden structures in Akungba-Akoko, Southwestern Nigeria. *International Journal of Science and Technology*, 2(1), 122-147.

Overbeek J., 1952, Electrochemistry of the double layer, in: H.R. Kruyt (Ed.), Colloid Science, 1, Irreversible Systems, *Elsevier, New York*, pp. 115.

Oversby, V. M. (1975). Lead isotopic study of aplites from the Precambrian basement rocks near Ibadan, southwestern Nigeria. Earth and Planetary Science Letters, 27(2), 177-180.

Revil, A., and Jardani, A. (2013). The self-potential method: Theory and applications in environmental geosciences. Cambridge University Press.

Satheeshkumar, S. (2024). Assessment of groundwater potential using 1D model of vertical electrical sounding and aquifer protective capacity in the Naraiyur micro-watershed. *Modeling Earth Systems and Environment*, *10*(1), 913-925. DOI: https://doi.org/10.1007/s40808-023-01819-x

Servin Vega, F. L. (2024). *Thermal activation of tunnel infrastructures: insights from three Italian case studies* (Doctoral dissertation, Politecnico di Torino).

Sunkari, E. D., Kore, B. M., and Abioui, M. (2021). Hydrogeophysical appraisal of groundwater potential in the fractured basement aquifer of the federal capital territory, Abuja, Nigeria. Results in Geophysical Sciences, 5, 100012. DOI: https://doi.org/10.1016/j.ringps.2021.

Tanko, I. Y., Adam, M., and Dambring, P. D. (2015). Field features and mode of emplacement of pegmatites of Keffi area, north central Nigeria. International Journal of Scientific & Technology Research, 4, 214-229.

Udosen, N. I., Ekanem, A. M., & George, N. J. (2024). Geophysical exploration to assess leachate percolation and aquifer protectivity within hydrogeological units at a major open dump in Eket, Nigeria. Results in Earth Sciences, 2, 100022. DOI: https://doi.org/10.1016/j.rines.2024.100022.

Wei, Y., Chen, Y., Cao, X., Xiang, M., Huang, Y., & Li, H. (2024). A critical review of groundwater table fluctuation: formation, effects on multifields, and contaminant behaviors in a soil and aquifer system. *Environmental Science & Technology*, *58*(5), 2185-2203.